

GENOMIC UNDERPINNING OF DROUGHT-ASSOCIATED PHENOTYPES IN A
KEYSTONE SHRUB SPECIES OF WESTERN NORTH AMERICA

by

Carlos Dave Contreras Dumaguit



A thesis

submitted in partial fulfillment

of the requirements for the degree of

Master of Science in Biology

Boise State University

August 2023

© 2023

Carlos Dave Contreras Dumaguit

ALL RIGHTS RESERVED

BOISE STATE UNIVERSITY GRADUATE COLLEGE

DEFENSE COMMITTEE AND FINAL READING APPROVALS

of the thesis submitted by

Carlos Dave Contreras Dumaguit

Thesis Title: GENOMIC UNDERPINNING OF DROUGHT-ASSOCIATED PHENOTYPES IN A KEYSTONE SHRUB SPECIES OF WESTERN NORTH AMERICA

Date of Final Oral Examination: 17 May 2023

The following individuals read and discussed the thesis submitted by student Carlos Dave C. Dumaguit and they evaluated the student's presentation and response to questions during the final oral examination. They found that the student passed the final oral examination.

Sven Buerki, Ph.D. Chair, Supervisory Committee

Stephen Novak, Ph.D. Member, Supervisory Committee

Marcelo Serpe, Ph.D. Member, Supervisory Committee

The final reading approval of the thesis was granted by Sven Buerki, Ph.D., Chair of the Supervisory Committee. The thesis was approved by the Graduate College.

DEDICATION

This thesis is dedicated to sagebrush.

ACKNOWLEDGMENTS

I would like to acknowledge the leadership and mentorship of Sven Buerki throughout my time in this program. I would also like to acknowledge the people that I have received massive support from during my time at Boise State University: my committee members and former instructors Stephen Novak and Marcelo Serpe, mentor and coffee enthusiast Anthony Melton, lab manager Peggy Martinez, lab colleagues and fellow students Michael Wojahn, Paige Ellestad, and Teo Geisler, Nicole Teregeyo and the staff within the Department of Biological Sciences, as well as friends, family, and others I have known who helped me in countless ways throughout my years of study.

ABSTRACT

Anthropogenic climate warming and habitat loss threaten species and ecosystem sustainability. Given this, it is urgent to determine whether populations can adapt at a rate sufficient to combat climate change or if human intervention is needed to preserve community ecosystem health. Assessing whether populations could adapt includes inferring whether key phenotypic traits associated to abiotic tolerance are under genetic control and therefore heritable. This thesis focused on the imperiled western North American sagebrush steppe and its widespread eponymous keystone species *Artemisia tridentata*, (common name, big sagebrush). To determine the adaptive capacity of any population, standing variation for phenotypic traits across its climatic range must be known, allowing for predictions of performance under climate change conditions. For sagebrush populations, we investigated phenotypic trait variation by examining leaf stomata density and size to infer water use efficiency as well as xylem diameter to infer relative risk of embolism, then used comparative genomic analyses to test for signature of natural selection driven by climatic conditions. A common garden greenhouse experiment included 41 seedlings from four populations from Idaho, Nevada, and Utah, sampled across a cline which represent a potential evapotranspiration gradient. If distinct phenotypes were observed under optimum conditions, then this would provide evidence for genetic control of these traits. Light microscopy observations to leaf epidermis and roots were used to record phenotypes associated with performance under drought stress and comparative statistical analysis was conducted to determine phenotypes at population

level. This study showed that seedlings from Utah exhibited significantly more dense stomata, a trait associated with increasing transpiration water loss, but greater allocation of large diameter xylem vessels, which would increase the risk of embolism. In contrast, seedlings from Idaho and Nevada exhibited significantly less stomata density, a trait known to decrease transpiration water loss, and greater allocation of small diameter xylem vessels mitigating risk of embolism. The genetic underpinning of phenotypes was investigated by reconstructing 12 individual genomes from three significantly different stomata phenotypes by applying a genome reconstruction approach using Illumina short reads. To test for the signature of local adaptation, single nucleotide polymorphisms were called and a PCA was conducted. The latter analysis returned the same climatic and phenotypic clustering as previously observed with Utah seedlings being separated from those from Idaho and Nevada. Combining phenotypic and genomic data support a hypothesis of genetically controlled phenotypic traits reflecting local adaptation. In all populations, individuals with less dense and smaller-sized stomata increasing drought tolerance as well as smaller diameter xylem with greater tolerance to embolism exist. Future work should explore gene expression responsible for phenotypic trait development under controlled drought, with continued work informing practices to improve ecosystem restoration of big sagebrush and maintenance of this keystone species in the face of climate change.

TABLE OF CONTENTS

DEDICATION	iv
ACKNOWLEDGMENTS	v
ABSTRACT.....	vi
TABLE OF CONTENTS.....	viii
LIST OF TABLES	xi
LIST OF FIGURES	xii
LIST OF ABBREVIATIONS.....	xv
CHAPTER ONE: MEASURING PHENOTYPIC TRAITS contributing to ADAPTIVE CAPACITY IN A KEYSTONE SPECIES IN THE SAGEBRUH STEPPE	1
Abstract	1
Introduction.....	2
Human driven climate change	2
Big sagebrush in the sagebrush steppe.....	4
Phenotypes of interest.....	5
Objectives & Hypotheses.....	8
Materials & Methods	9
Climate Analysis.....	9
Greenhouse Common Garden Experiment	11
Leaf Sampling.....	12
Leaf Phenotyping	13
Root Sampling	14
Statistical Analyses	15

Results.....	16
Sampling.....	16
Biomass.....	16
Carbon Isotope Analysis.....	17
Leaf Area.....	17
Comparing Leaf Surfaces.....	17
Stomata Density.....	18
Stomata Size.....	18
Endoderm Area.....	18
Observation of Concavities.....	19
Xylem Diameter Allocation.....	19
Discussion.....	20
Phenotypic Observations in Common Garden Seedlings.....	20
Further Work.....	27
CHAPTER TWO: DETERMINING GENETIC UNDERPINNING OF PHENOTYPIC DIFFERENCES OBSERVED FROM A STUDY OF SAGEBRUSH SEEDLINGS.....	30
Abstract.....	30
Introduction.....	31
Genomics in the Age of Climate Change.....	31
Summary of Previous Phenotypic Research.....	33
Objectives & Hypotheses.....	34
Methods.....	35
Sampling.....	35
DNA Extraction & Resequencing.....	35

Bioinformatics.....	35
Analyses.....	36
Results.....	37
Sampling for DNA Extraction	37
Genomic Dataset.....	38
Analyses.....	38
Discussion.....	39
Genomic Data	39
Future Research	43
APPENDIX A.....	47
TABLES	49
FIGURES.....	52
REFERENCES	66

LIST OF TABLES

Table 1.1	Sampled populations for greenhouse common garden.	49
Table 2.1	Table of seedlings sampled for genome resequencing.	49
Table 2.2	Raw sequencing data statistics.....	50
Table 2.3	Read trimming data statistics.....	50
Table 2.4	Level of heterozygosity per individual	50

LIST OF FIGURES

Figure A.1	Map of sagebrush populations 1	48
Figure 1.1	Microscopic images of sagebrush leaf (<i>Artemisia tridentata</i> ssp. <i>tridentata</i>). LEFT. Transverse cross section of a sagebrush leaf. Note the presence of green photosynthesizing palisade cells interior to both epidermis layers. Sagebrush leaves have an isobilateral amphistomatous structure, allowing for high conductance of CO ₂ and shorter distance of gas diffusion utilizing stomata found on both surfaces. RIGHT. Image of leaf epidermis resulting from stomatal assay protocol. Taken at 400x magnification.	52
Figure 1.2	Half-violin-boxplot comparing biomass (grams) across populations of identically grown greenhouse sagebrush seedlings (<i>Artemisia tridentata</i> spp. <i>tridentata</i>). Populations are arranged in increasing PET value. Total plant biomass showed variation under identical optimum greenhouse conditions. A Kruskal-Wallis test returned a statistically significant effect of at least one population's distribution over the others (p-value < 2.2e-16). However, a post hoc Dunn's test looking at pairs of populations did not return any significant pairwise contrasts.	53
Figure 1.3	Half-violin-boxplots of carbon isotope ratios among identically grown greenhouse sagebrush seedlings. A GLM returned no statistically significant differences at the population level ($\alpha < 0.05$). From this, we can infer that the water use efficiency (WUE) of all our seedlings were similar, with all experiencing the same lack of water stress when combined with our well-watered conditions.....	54
Figure 1.4	Boxplot of leaf areas from sampled sagebrush seedlings. A generalized linear model (GLM) returned a significant population effect (p-value = 0.0577; $\alpha < 0.05$).....	54
Figure 1.5	Half-violin-boxplot comparing stomata characteristics between adaxial (top) and abaxial (bottom) surfaces in sagebrush leaves. No statistically significant differences were found between leaf surfaces ($\alpha < 0.05$), allowing for downstream phenotype analysis. A. Two leaves were sampled from 41 plants, each representing data from one leaf surface. Three identically sized viewing windows (six per seedling) were counted for stomata density calculations. B. Four stomata were measured for every viewing window (24 per seedling) for stomata size calculations.	55

Figure 1.6 Half-violin-boxplot comparing stomata characteristics across sampled populations of sagebrush seedlings. RED denotes populations found within the ALPHA cluster (populations IDT3, IDT1, & NVW1) from a previous climatic principal component analysis (PCA) while BLUE denotes inclusion within the BETA cluster (population UTT2). A. Stomata density showed variation and statistically significant differences at the population level. B. Stomata size also showed variation and statistically significant differences at the population level. 56

Figure 1.7 Half-violin-boxplot comparing area of encapsulated by the endoderm at the population level. Measurements were taken at the crown of each seedling, the widest and oldest area of vasculature. Seedlings’ endoderm areas did not show any population effect, translating to similar amounts of transverse cross-sectional area of endoderm tissue across all populations. 57

Figure 1.8 Image of transverse cross-section of sagebrush seedling 0099. Note the presence of damage to the vascular cambium as outlined in red. These areas are void of vascular tissue, as opposed to being part of a continuous unbroken area in the shape of a circle. Larger light blue circles in the bottom of the image are xylem while the smaller richer blue circles that have taken dye are phloem cells. 58

Figure 1.9 Bar plots of xylem allocation at diameter intervals across sampled sagebrush populations. Population IDT3 showed the largest percentage allocation to large diameter vessels compared to other populations, increasing risk of embolism during drought conditions. 59

Figure 2.1 Example dot plot analysis output comparing re-sequenced individuals to reference genome. Shown above is the plot for sample 379, *Artemisia tridentata* ssp. *tridentata* from population NVW1 in Nevada. All dot plot analyses inferred high similarity across all pseudo-chromosome scaffolds, as can be seen by the unbroken diagonal line and less than 1% difference found at all levels. There were also no large chromosomal rearrangements. The rest of the samples’ dot plots can be found in supplementary material. 60

Figure 2.2 Genome coverage map comparing sample 379 with the reference genome. No large chromosomal rearrangements were found. All samples were found to have similar plots with appropriate genome coverage. The other samples’ coverage maps can be found in supplementary materials..... 61

Figure 2.3 Heatmap comparing samples with the reference genome at the pseudo-chromosome level. We found high levels of similarity between the reference genome and all samples; less than 1% difference was inferred. Samples did not segregate directly into populations..... 62

Figure 2.4 Principal Component Analysis (PCA) of filtered biallelic single nucleotide polymorphisms (SNPs) of diploid basin sagebrush seedlings (*Artemisia tridentata* ssp. *tridentata*). The top eigenvector segregated our twelve seedlings following the same division as previous climatic and phenotypic analyses at the population level. 63

Figure 2.5 Dendrogram with bootstrap support showing genetic distance differentiation. Sample IDs are at the terminal ends of branches. Genetic differentiation was calculated using Nei's distance (1987). Branching between seedlings from population UTT2 and the rest was supported- bootstrap value 100. 64

Figure 2.6 Cross Entropy plot output from STRUCTURE analysis. The STRUCTURE analysis indicated that one ancestral meta-population was the most likely scenario to explain the neutral SNP variation in our dataset, as seen by scenario 1 having the lowest cross-entropy value..... 65

LIST OF ABBREVIATIONS

PET	Potential evapotranspiration
WUE	Water use efficiency
SNP	Single nucleotide polymorphism
PCA	Principal component analysis
GLM	Generalized linear model
DNA	Deoxyribonucleic acid

CHAPTER ONE: MEASURING PHENOTYPIC TRAITS contributing to ADAPTIVE
CAPACITY IN A KEYSTONE SPECIES IN THE SAGEBRUH STEPPE

Abstract

In the sagebrush steppe of North America, *Artemisia tridentata* or big sagebrush, is a keystone species under threat by many factors including climate change and drought. To aid efforts in its conservation and restoration, we need to understand population adaptive capacity, defined as their ability to respond at a rate sufficient to combat climate change. We hypothesized that populations of sagebrush have undergone local adaptation related to a climatic gradient of potential evapotranspiration (PET), a measure of water demands in the landscape. Based on literature, we predicted that sagebrush seedlings in higher PET environments would display smaller, less dense stomata to minimize water transpiration loss and smaller diameter vessels to mitigate risk of vessel cavitation due to their more stressful local climate. Seedlings were sampled from four populations and then grown for two years in identical well-watered conditions in a greenhouse common garden experiment. Stomata phenotyping revealed significant differences in stomata density and size between populations, with seedlings from sites with lower potential evapotranspiration displaying lower stomatal density. Xylem phenotyping also revealed significant differences, with seedlings from Utah exposed to the North American monsoon, having greater allocation of small diameter vessels. These results point to individuals that are pre-adapted to climate warming projections. Future genotyping should identify genes that might underpin these adaptive phenotypes.

Introduction

Human driven climate change

Anthropogenic climate change is a global crisis threatening ecosystems and biodiversity. Mean temperatures are rising at an increasing rate, multiplying extreme climate events (Intergovernmental Panel on Climate Change [IPCC], 2022; Xu et al., 2018). In North America, the last two decades have been the longest stretch of megadrought, a consequence directly attributed to human activity (Stahle, 2020; Williams et al., 2020). Coupled with human land use change, many species are in decline, nearing or reaching extinction (IPCC, 2022). Significant corrective measures are needed to curtail these losses, especially as trends point to increasing extinctions in the coming decades (IPCC, 2022; IUCN, 2020). To create actionable and effective conservation and restoration policies, policymakers must accurately understand ecosystem exposure to climate threats and an ecosystem's level of vulnerability followed by an assessment of adaptive capacity to respond to these threats (Ofori et al., 2017). Using this framework such as outlined by the climate change vulnerability assessment researchers can put forth hypotheses and produce experiments to give policy makers evidence to support measures protecting biodiversity.

Adaptive capacity is a measure of the potential of a species or populations of a species to tolerate or adapt to climate change (Ofori et al., 2017). It is made of three components, one of which is the potential to undergo microevolution, changing their frequency of alleles (Ofori et al., 2017). Similar to studying macro-evolution on the species scale and evolutionary time frame, the first step is observing variation in a heritable phenotype (Franks & Hoffman, 2012). In microevolution, changes occur on

relatively shorter time scales. In the example of Methicillin resistant staphylococcus aureus, colonies of bacteria can generate in a matter of days. The frequency of alleles increasing survival can increase rapidly due to natural selection via constant dosages of antibiotics (CDC-PHL). Phenotypic variation such as with differential resistance to antibiotics can exist as a direct result of genetic variation in a population, often investigated by looking at genetic markers like single nucleotide polymorphisms (SNPs). A second component to adaptive capacity is phenotypic plasticity- traits that change based on the current environment within an individual's lifespan. This has been observed in soybean and maize plants undergoing water stress resulting in decreased leaf and stomata size (Mano, Madore, & Mickelbart, 2023). Phenotypic plasticity can confer fitness gains as temperatures increase, but eventually environmental stressors will be far too great for plastic variation to sufficiently overcome. The third component of adaptive capacity is dispersal, the ability of a species to leave their current in order to track their niche and remain in a suitable growing environment (Ofori et al., 2017). This ability is lessened in plants when compared to animals due to their sessile nature once they have colonized a location, necessitating dispersal by movement of offspring.

One pool of variation to explore is the trait differences in populations due to local adaptation (Aitken et al., 2008). In *Arabidopsis thaliana*, Dittberner et al. (2018) found evidence for local adaptation influenced by local population climate; variation in leaf stomata traits conferred different water use efficiencies mirroring geographic distribution and climate. Differences in drought stress over time selected for more adaptive characteristics, shaping genetically controlled phenotypic trait variation across its range. Stojnic et al. (2018) observed variation in vascular tissue in European beech tree

populations conferring differential resistances to aridity in certain marginal populations across its range, which experienced dryer climates. Given enough time under reproductive isolation from other populations, a climatic gradient in the landscape can select for variation in traits specific to each cline that populations are located along (Rumman et al., 2017). In the framework of adaptive capacity, conservation ecologists can aim to find populations displaying variation, hopefully containing some traits more adapted to stressful drought conditions and inform restoration efforts to prioritize their propagation to supplement struggling, less adapted populations.

Policies concerning climate actions should focus on the most threatened species with disproportionately greater impact on ecosystems (Urban et al., 2016). In the rangelands of North America, big sagebrush, or *Artemisia tridentata* is a keystone species exposed to increasing drought conditions, coupled with many factors such as wildfire creating unsuitable, novel environments. These threats necessitate a genome to phenome approach gain a better understanding of sagebrush populations in order to reverse a history of markedly unsuccessful efforts of conservation and restoration. Although uncommon, a research project combining climatic niche analysis, genotyping-by-sequencing, and phenotyping common garden individuals can effectively answer these queries into population adaptive capacity (Faske et al., 2021).

Big sagebrush in the sagebrush steppe

Big sagebrush (*Artemisia tridentata*) is a keystone plant species of the sagebrush steppe ecosystems. These ecosystems span numerous states in the U.S. and Canada with sagebrush individuals present in over a million square kilometers of rangeland in North America (Rigge et al., 2020). These shrubs support many obligate species such as sage

thrasher, pygmy rabbit, and sage-grouse (Knick et al., 2003; Remington et al., 2021). Over the past century, the sagebrush steppe has been exposed to human land use change, overgrazing, plant invasions, and alteration of fire regimes, all exacerbated by anthropogenic climate warming (Xu et al., 2018; Coop et al., 2020; Stahle, 2020; Williams et al., 2020). These threats create a novel habitat affecting seedling recruitment and ultimately causing population decline across big sagebrush's large historic range (Coop et al., 2020; Perryman et al., 2000). Observations of sagebrush stands have shown seedlings are only successful in favorable climatic conditions such as high precipitation years. Over the past 75 years, the occurrence of a successful recruitment year was between 37% and 59% depending on subspecies, patterned between years of zero recruitment survival (Maier et al., 2001; Perryman et al., 2000). Seedling recruitment is essential for maintaining populations and allowing population recovery following disturbance. Measuring the potential of big sagebrush populations to adapt to climate change at this life-cycle stage should be prioritized. With climate projections predicting more frequent and intense drought across North America, phenotypes related to how seedlings efficiently utilize water are paramount, especially if these phenotypes confer higher chances of survival during less favorable years of precipitation. With that in mind, I chose to investigate phenotypic variation in stomata and xylem, key structures in how plants manage their water use.

Phenotypes of interest

Plants use a variety of strategies to conserve water levels while maintaining essential plant functions during drought stress. A commonly used physiological measurement in assessing these plant strategies is water use efficiency (WUE), directly

impacted by leaf stomata, the avenue through which gases essential for photosynthesis move into the leaf. A higher rate of carbon dioxide diffusion while minimizing water lost through transpiration will yield higher WUE, both of which are constrained by the phenotypic characteristics of stomata (Meng, 2018; Bertolino et al., 2019; Gupta et al., 2020; Franks et al., 2015). Variation in stomata can include differences in their density, size, and patterning (Faralli et al., 2019). A theoretical plant with highly efficient stomata will have high stomata density, small stomata size, and spread patterning without clusters. These characteristics maximize the diffusion rate of carbon dioxide and minimize the time it takes to close thus reducing water loss. However, many factors affect the adaptiveness of these characteristics as such the photosynthetic rate ceiling. Varying levels of drought stress will also necessitate faster closing or less dense stomata to balance carbon dioxide intake and transpiration for higher WUE.

In select literature, a reduction in stomatal density has been observed to increase WUE in many species including *Arabidopsis thaliana*, bread wheat, *Oryza sativa*, poplar conifers, and *Zea mays* (Dunn et al., 2019; Hughes et al., 2017; Kardiman & Raebild, 2018; Franks et al., 2015; Wang et al., 2012; Zhang et al., 2012). The reduction in density decreases the amount of water lost through transpiration without affecting the photosynthetic yield. In natural populations, populations with variation in stomata density will in turn have variation in WUE; selecting for the plants with the lowest average density should theoretically yield the highest WUE, as was the case in different strains of rice and Sumatran rainforest tree species (Kardiman & Raebild, 2018).

Stomata impact water use above ground, but drought also affects structures below ground before water reaches the stomata in leaves. Under drought, vessels carrying water

upward from the roots can develop pockets of air that disrupt the water column, resulting in embolism that leads to vessel cavitation. Excessive cavitation causes plant death as they can no longer maintain water continuity along the xylem, preventing the upward movement of water (Schenk, 1999). Reduction in embolism was observed in beech tree populations with varying climatic conditions, suggesting that small differences in climatic stressors are sufficient for local adaptation in this trait (Stojnic et al., 2018). One strategy that has evolved to reduce cavitation is the reduction in xylem vessel diameter, having been shown to reduce embolism in various tree species (McElrone et al., 2004).

Other shrub species throughout the world exhibit consistent tissue loss in their vasculature tissue, allowing for compartmentalization of vessels, referred to as clonal splitting by Schenk (1999). Ginzburg (1963) observed these anatomical anomalies in desert shrubs in the Middle East, noting them in an *Artemisia* species *Artemisia herba-alba*. In water abundant environments, this modular development impedes maximal growth, as water taken in by the roots is not evenly distributed throughout the above-ground structures. However, in desert conditions, this modularity protects areas of the plant, preventing the whole plant from dying via vascular tissue cavitation, spreading this risk to independent 'ramets' (Schenk, 1999). One 'module' that is hydraulic independent is sacrificed for the survival of the rest of the shrub (Schenk et al., 2008). Abnormalities in *Artemisia tridentata* root cross sections have been observed previously but further confirmation is needed within the larger context of adaptive hydraulic independence (Evans et al., 2019).

Objectives & Hypotheses

My first hypothesis concerned the amphistomatous nature (i.e., stomata are on both the upper and lower leaf surfaces) of sagebrush leaves, a characteristic that has been confirmed but not targeted specifically for density and size observations for both leaf surfaces (Downs & Black, 1999). We hypothesized that sagebrush leaves are isobilateral amphistomatous in nature, with patterning of stomata on both sides due to their near vertical phyllotaxy for low angle light capture during periods of less severe heat and light intensity during the day. This is ideal for light capture during the median hours of day light with the sun directly overhead, without a direct line at stomata.

A greenhouse common garden experiment planned to grow seedlings without water stress. We hypothesized that by exposing seedlings to well-watered conditions, they should all develop without drought or water stress. Without environmental limitations, we predict all seedlings should all maximize photosynthesis and accumulate the same amount of biomass and exhibit similar carbon isotope ratios which are indicative of intrinsic WUE.

I hypothesized that if local adaptation occurred in sagebrush, then seedlings from populations with the highest PET value should have been selected to exhibit the lowest stomata density to reduce transpiration while maintaining photosynthesis, consistent with previous research findings (Faralli et al., 2019; Dunn et al., 2019; Hughes et al., 2017; Kardiman & Raebild, 2018; Franks et al., 2015; Wang et al., 2012; Zhang et al., 2012). I also hypothesized that seedlings from the same high PET location would exhibit the smallest stomata size, allowing for rapid stomatal closure in response to abiotic stress.

Regarding vascular phenotype, I hypothesized that seedlings from the location with the highest PET would be enriched in vessels most protected against xylem embolism and cavitation. While reducing hydraulic conductivity, this trait would minimize risk of embolism and hydraulic failure. Along with the vessel diameter allocation, I hypothesized that concavities would be enriched in seedlings from the highest PET location, indicating a propensity for clonal splitting, therefore transitioning from integrated to modular hydraulic redundancy, reducing whole plant mortality by cavitation.

Materials & Methods

Climate Analysis

To sample populations for an assessment of local adaptation, we analyzed climate variables from the locations where our seed samples were generated. Climate data from WorldClim and CGIAR CSI, was downloaded and extracted using R package ‘raster’ (Available at: <https://cran.r-project.org/package=raster>) for a dataset of climatic variables. This data was downloaded at 30 arcsec resolution (~1km at the equator). Point data was overlapped with R package ‘raster’ to extract climate data for each sample location. These climate variables were used for a principal component analysis (PCA) and clustering analysis, which returned two clusters best explained by potential evapotranspiration (PET) and elevation (Melton et al., 2023 [IN REVIEW]). The variable PET has been used to quantify the atmospheric demand for water in the landscape (Lu et al., 2005). Previous literature noted that 80 – 93% of the variability in species richness can be explained by ecosystem PET (Lu et al., 2005).

Four sample locations were the focus of this experiment. Seeds were provided by Bryce Richardson, USGS, and their use and identification coincide with previous work on sagebrush diversity and ploidy (Richardson et al., 2012). Each seedling was a known diploid of *Artemisia tridentata* ssp. *tridentata* from populations labeled by state, subspecies, and number: IDT1 (43.0962, -115.657), IDT3 (43.3366, -116.964), NVW1 (41.5147, -117.775), and UTT2 (38.306, -109.388). Note that NVW1 is labeled 'W' previously misidentified as polyploid subspecies *wyomingensis* due to previous predictions, however, it is a known diploid subspecies *tridentata*. The naming convention remains to maintain reproducibility with previous studies. These four locations represent a climatic gradient of PET, in increasing order: IDT3, IDT1, NVW1, and UTT2, (1537, 1655, 1767, 1790 $\frac{mm}{day}$ respectively). In the past, dryland ecosystems have been identified in the past using PET, and here we rank our sample locations based on PET to contextualize their relative level of drought stress during the seasonal drought occurring immediately after the wet growing season in the Spring.

Population IDT3 is within climatic cluster ALPHA, the sample location experiencing the lowest PET. Population UTT2 is the representative sample location for the cluster BETA, experiencing the highest PET. Sample location NVW1 is climatically and geographically intermediate between IDT3 & UTT2. Sample location IDT1 is also an intermediate location and is a known site of restoration. Although IDT1 is within the cluster ALPHA, the plants at this location were restored with seedlings or were seeded from a source found in Utah which means that population is likely a mix of seedlings from both climatic clusters.

Greenhouse Common Garden Experiment

Seeds from the four populations were grown in a common garden greenhouse experiment. Bryce Richardson of the US Forest Service provided seeds from ten maternal plants from each population. These seeds were planted on July 10, 2019, in the research greenhouse on the Boise State University campus Boise, Idaho, USA (43.615833, -116.201667).

A common garden experiment was chosen as the ideal way to analyze big sagebrush due to the range of climates across the species' range. Although similar, our experiment differs from a reciprocal transplant experiment as we are not directly testing for competing fitness in differing environments, instead opting to grow all our seedlings in the same optimum environment. This approach allows us to observe occurrence of phenotypic variation from known geographic and climatic variation from our sampled populations (Aitken et al., 2008; de Villemereuil et al., 2016; Faske et al., 2021). We analyzed one individual from each of the ten mother plants in order to observe genetic and phenotypic variation within each population as well as variation at the population level.

As a non-model organism, resources to growing our study species are limited and need to be uniquely adapted from existing resources not purpose built to study sagebrush. Phenotyping of individuals in the field was not considered due to many confounding variables in the environment. By growing all the seedlings in the same environment, we also minimized impact of maternal effects with a two-year growing process. The two years of growth before sampling also ensured that leaves were adapted to their environment.

Conditions in the greenhouse were maintained at 20°C with a day-night cycle of 16:8 hours. Watering occurred on alternating days to avoid oversaturation of soils. Every two weeks, racks holding groups of seedlings were shuffled randomly to a new position on greenhouse benches to minimize greenhouse microclimate effects. Many seeds were started but thinning ensured only one plant survived per container and one individual survived per mother plant (Navock, 2020). The ideal plant for phenotype sampling displayed seedling traits consistent with tridentate leaves with a dark sage-green sheen, indicating photosynthetic capability was attained. After two years of growth, individuals utilized for phenotyping were cleaned, dried, and prepared for herbarium storage.

To ensure that our seedlings were grown under identical well-watered conditions, a carbon ratio isotope analysis was conducted. This procedure has been used in multiple species to delineate between plants that were under water stress compared to plants that had ample water resources (Hartman and Danin, 2010). Tissue samples were taken from 40 of the preserved seedlings. Carbon isotope analysis was conducted by a stable isotope facility at Boise State University (Reynard Lab, Stable Isotope Laboratory, Department of Geosciences).

Leaf Sampling

Leaves were sampled in the morning when stomata are open for photosynthesis. Two leaves were chosen from each individual for stomata phenotyping due to the destructive nature of our protocol. One was used solely for the abaxial surface and one for the adaxial, choosing leaves from the upper third of the main stem of each seedling to prioritize developed leaves undergoing photosynthesis, avoiding possible immature or ephemeral leaves. Two more leaves were chosen under the same procedure for leaf area

analysis. A protocol was developed to observe the epidermal layer of the leaves using light microscopy. We based this protocol on work done on other plants for stomata experiments (Allsman et al., 2019; Eisele et al., 2016; Wu et al., 2009; da Silva et al., 2016). Briefly, this newly generated protocol sampled seedling leaves and removed the trichome hairs found on the surface. High strength adhesive was applied directly onto the leaf surface with tape immediately following creating a sandwiched layer of glue which, when the tape was gently removed, the leaf epidermis was peeled off, allowing for direct observation of stomata. After above ground phenotype analysis, the seedlings were dried and preserved for later root phenotyping and genetic analyses. The plants were uprooted, cleaned, pressed, and dried for herbarium storage.

Leaf Phenotyping

Leaf area images were processed into pixelized outlines of each leaf and area was estimated from these processed images in R using user defined functions. Images of leaves for stomata phenotyping were taken on a Leica model CME microscope with images captured by a Motic Moticom X3 microscope camera. The imaging device was calibrated with provided stage micrometer slides prior to imaging. Previous research on stomata in other plant species has noted the variation in stomata characteristics when comparing areas of leaves between plants of the same species, among leaves of the same plant, and even among different areas of the same leaf (Slavik, 1963; Pazourek, 1973; Bimova, 1992). We modeled our protocol on a random sampling protocol by Kubinova (1994) which aimed to maintain comparability for stomata phenotyping due to this variation. Three images at 10x objective lens were captured on each surface of every leaf. These images were used to gather stomata density data. Two more images were taken at

40x objective lens within the confines of each 10x image. These two images focused on capturing higher resolution examples of stomata for dimension measurements. In total, for each individual seedling, this created a dataset of 6 images for stomatal density measurements and 12 images for stomatal size measurements.

Stomata data were gathered by hand due to a lack of compatible automated programs that could distinguish sagebrush stomata accurately. Light microscope images of leaves were first processed in R to standardize size and add grid markings to each image for scoring. Count data was gathered within a 1000 um X 600 um area, recording data in Microsoft Excel for each sample. Measurements of stomata dimensions were gathered using the vector line tool within image software FIJI/ImageJ (Schindelin et al., 2019) using the 40x images. To accurately measure stomata size, guard cell length was measured from end to end. Measuring only diameter was inaccurate due to differences in angle of stomata along the uneven surface of the epidermis.

Root Sampling

After specimen preservation, root cross sections were obtained with xylem cross sections sliced from a section of root within the first 2.5 cm below the crown of each seedling, determined by the visible soil line. Dried roots were soaked in water and cross sections were cut and dyed with toluidine blue. Cross sections were viewed and imaged in a light microscope. Some xylem vessel imaging required multiple images to fully capture the entire area containing vessels in clear focus. Images were then combined using image editing software Adobe Illustrator.

Xylem vessel phenotyping data was gathered by hand as no programs existed at the time for distinguishing vascular tissue cross sections for non-model organisms. Using

the image tool FIJI/ImageJ, diameters of xylem vessels were measured with the vector tool. Measurements were calibrated based on the image's scaled ruler that was calibrated for imaging in the same manner as leaf phenotyping previously. Specific count data was derived from the number of measurements. Only one quadrant (90 degrees) of total cross section area was counted due to unreliable whole image quality and time constraints.

Previous findings have observed concavities in the vascular cambium in sagebrush (Evans and Graney, 2018). We chose to investigate this by estimating the amount of vascular area that has died in the taproot due to concavities. To analyze total vascular cross-sectional area of each seedling, polygon outlines of the vascular cambium containing vessels were drawn in ImageJ. Predicted maximal growth of vascular tissue was estimated calculating a theoretical circle of growth using the largest diameter line that could be measured of the vascular cambium.

Statistical Analyses

Preliminary data sets were tested for distribution using the Shapiro-Wilk test; most data were not normally distributed. Non-parametric tests were chosen to analyze our data. When investigating population level differences, a Generalized Linear Model (GLM) or Kruskal-Wallis test was conducted. The latter was used when comparing the biomass dataset due to the differences in distribution among populations. If the models had statistical significance, a post-hoc Tukey test or Dunn's test was conducted to compare each population in pairs. The latter test was used in conjunction to the Kruskal-Wallis test. A statistical significance threshold at $\alpha \leq 0.05$ was chosen, denoted as a single asterisk (*). For GLMs, significant intercept values were not considered relevant, as phenotype data measurements were always greater than 0.

Results

Sampling

Forty-one seedlings were analyzed for leaf phenotypes, with 10 individuals each from populations IDT1, IDT3, and NVW1, while 11 individuals were analyzed from population UTT2 (Table 1.1). The additional seedling analyzed for population UTT2 was accidental. For root phenotype analysis, 35 seedlings were fully preserved and sampled for analysis, with nine individuals for the IDT1, IDT3, and UTT2 populations, and eight individuals from the NVW1 population (Table 1.1). Sampling of leaves occurred between June and July 2021. Subsequently, seedlings were preserved, and biomass data was measured in early July of 2021, with root phenotyping occurring in August of 2021. Some preserved seedlings had roots that were too fragile or damaged prior to cross section imaging procedures and did not yield suitable images for data gathering. With cross sections of leaves on the transverse plane, we were able to confirm that sagebrush leaves are isobilateral and amphistomatous in structure (Drake et al., 2013). Stomata were seen on both abaxial and adaxial leaf surfaces. A transverse cross section of leaves showed two layers of green palisade cells (Figure 1.1).

Biomass

Biomass measurements were taken after all greenhouse-grown seedlings were taken for preservation as herbarium specimens. The distributions of biomass varied across populations from a more limited range of values in population IDT3 and wider range of biomass values in the other three populations (Figure 1.2). A Kruskal-Wallis test (Kruskal & Wallis, 1952) was used to analyze variance with respect to these distributions, returning a significant p value (p -value $< 2.2e-16$). My dataset appears to be

ordered in relation to at least one population. When comparing between two populations, a Dunn's test did not return any comparisons below an adjusted alpha value of 0.05.

Carbon Isotope Analysis

A GLM analysis found no significant differences in carbon isotope ratios across the four populations (Figure 1.3). All carbon isotope ratio values occurred below the value of -26, consistent with previous research which saw similar values in other C3 plants growing without water stress (Hartman and Danin, 2009).

Leaf Area

A GLM found significant differences in leaf area at the population level (Figure 1.4; p -value = 0.00153). A post hoc Tukey test for pairwise contrasts indicated that UTT2 had greater mean leaf area than IDT1 and NVW1 (p -value = 0.0056; p -value = 0.0432). This difference in leaf surface area was controlled for density analysis by standardizing the amount of surface area measured. For density of stomata, images were cropped to sections measuring 1000 μm by 600 μm .

Comparing Leaf Surfaces

Using the images from the leaf stomata assays, we aggregated the data at the surface level (Figure 1.5). The datasets for stomata densities and dimensions were not normally distributed based on the Shapiro-Wilk test for normality (p -value = 0.0006709, stomata density; p -value = 0.04577, stomata dimension). Leaf stomata density did not significantly differ between adaxial and abaxial surfaces across all samples (p -value = 0.338). Leaf stomata dimensions did not significantly differ between adaxial and abaxial surfaces (p -value = 0.565). Based on these results, the adaxial and abaxial surface datasets were merged into one dataset for further analysis at the population level.

Stomata Density

Density of stomata showed variation within each population. Analysis using a GLM returned populations IDT3* and UTT2*** (Figure 1.6A) as statistically different from the other populations (p -value = 0.0409, IDT3; p -value = 0.000202, UTT2). In a post hoc Tukey test for pairwise contrasts between populations, IDT3 showed significantly less stomata density than UTT2 (p -value = 0.0012). Population NVW1 also had significantly less stomata density when compared to UTT2 (p -value = 0.0227). Population UTT2 had a mean stomata density of 124.17 stomata per square millimeter compared to NVW1 with the lowest density of 95 stomata per square millimeter.

Stomata Size

Stomata size showed variation (Figure 1.6B). A GLM returned statistically significant differences in stomata size for IDT1*** and NVW1*** (p -value = 2.26e-06, IDT1; p -value = 3.66e-05, NVW1). A post hoc Tukey test for pairwise contrasts returned two groupings with two populations in each. The two populations in each group were not significantly different from each other, but each was significantly different from both populations in the other grouping. Populations IDT3 and UTT2 have smaller stomata size on average compared to populations ITD1 and NVW1 which have relatively larger stomata size.

Endoderm Area

Taproot cross section images were processed to include the entire area of vessels. Some xylem cross sections were stitched together to form a composite image using image software 'Adobe Illustrator' due to the large diameter of some taproots which were not wholly captured in a single image's field of view in the microscope. There was no

significant difference in vascular tissue cross sectional area between populations (Figure 1.7). This allowed us to compare the xylem diameter dataset between populations, as each population was allocating the same amount of cross-sectional area to vascular tissue.

Observation of Concavities

We observed concavities in the vascular bundle of nearly all samples. Many samples had an endodermis with sharp inward ‘V’ shaped concavities, far from the typical circular shape in most plant roots (Figure 1.8).

Measurements of tissue lost to concavities were calculated by subtracting observed area encompassed by the endodermis from maximal growth area estimate. The maximal growth estimate was calculated for each seedling by calculating the area of a perfect circle using the diameter of the largest observed diameter line in the imaged vascular cambium. A GLM returned a statistically significant intercept ($\Pr(>|t|) = 1.14e-5$). A post hoc Tukey test did not return statistically significant pairwise contrasts.

Xylem Diameter Allocation

For all cross sections, only 25% of the total area of vessels was measured, equivalent to a 90-degree section for each bundle sheath which resembled a circle. This was done to avoid discrepancies in measuring endoderm tissue that was significantly impacted by concavities/vascular tissue abnormalities. After data collection, the exact measurements were sorted into bins which comprised of seven bins spanning five micrometers of measurements. This process of turning the raw data into semi-quantitative data was done to match previous work on xylem anatomy, hydraulic efficiency, and cavitation risk (McElrone et al., 2004).

A GLM reported that populations showed differing allocations of xylem diameter per size class, with statistical significance in the model's intercept ($\text{Pr}(>|t|) = < 2e-16$), population NVW1 ($\text{Pr}(>|t|) = 1.32e-06$), and population UTT2 ($\text{Pr}(>|t|) = 2.33e-15$) (Figure 1.9). A post hoc Tukey test returned significant pairwise contrasts for all populations comparisons except between IDT1 and IDT3. Looking at proportions of vessels in each class, IDT3 was the only population that devoted over 50% of their total vessels to diameter greater than 5 micrometers. The rest of the populations had less than 50% allocation to the same class of vessels. Population IDT3 had 443 vessels at the 5-um class, while IDT1, NVW1, and UTT2 had 787, 634, and 734 vessels respectively.

Discussion

Phenotypic Observations in Common Garden Seedlings

To prevent consequential losses in biodiversity and ecosystems, efficient and effective interventions are needed to protect populations of keystone organisms. Policies hoping to reverse these losses should be informed with genome to phenome research to ensure the species populations most at risk are prioritized based on their lack of capacity to respond. At the heart of genome to phenome work is exploring variation across populations. In this project, we were able to observe variation in sampled populations of a threatened keystone species of sagebrush pointing to local adaptation.

Amphistomatous nature of leaves

Researchers target leaf phenotypes such as stomata for research into water use efficiency in crops and model organisms. Unfortunately, our study species posed problems for directly implementing existing protocols investigating leaf structures due to the size, shape, and fragility of sagebrush seedling leaves. To combat these factors, we

adapted protocols involving epidermis peeling, attempting different techniques and materials from glue impressions to adhesive peels. We settled on a repeatable and cost-effective protocol utilizing tape and strong adhesive to peel the leaf epidermis and directly observe stomata characteristics (See stomatal assay protocol). A previous study used electron microscopy to observe sagebrush leaf surface stomata and trichomes (Downs & Black, 1999). Our imaging is the first to reveal the epidermis layer without the obstruction of trichomes. For every seedling sampled, we observed stomata on both adaxial and abaxial leaf surfaces (Figure 1.1). In a transverse cross-section image (Figure 1.1), we also observed green photosynthetic palisade cells on both sides of the leaf, confirming an isobilateral amphistomatous structure for sagebrush leaves. Plants avoid drought stress by closing their stomata when heat is high to reduce water lost through transpiration, but commonly only have one ideal angle for photosynthesis due to phyllotaxy and stomata located solely on the abaxial surface (Fang & Xiong, 2015; Gupta et al., 2020). Having two photosynthetic cells behind both leaf surfaces adds evidence to support the hypothesis that sagebrush is able to take advantage of low angle light at the beginning and end of daylight hours when temperatures and light are less intense compared to direct overhead sunlight in the middle of the day. Stomata opposite the path of sunlight can be open twice a day allowing for gas exchange and photosynthesis, increasing their output of food stores but minimizing their water loss. Having stomata at both ends also reduces the distance gas travels when exiting the leaf, improving gas diffusion rates (Faralli et al., 2019).

Ensuring comparable individuals

Before we could investigate differences in seedling leaf stomata phenotype characteristics, we had to ensure our plants were comparable across populations as a result of our greenhouse protocol. Our greenhouse common garden experiment gathered seeds from populations with different local climates in one identical optimum growth environment. Seedlings were regularly watered to prevent water stress in a climate-controlled greenhouse. Pots were also shuffled among shelf positions to control for location effects within the greenhouse.

After two years of growth, we observed populations UTT2 and NVW1 had significantly different biomass (Figure 1.2). In aggregate, there was a population effect, but a lack of significant pairwise comparisons. This might be a signal that some seedlings had different growth conditions, however, there were large overlaps in range and outliers in all populations. More importantly, our carbon isotope ratio analysis (Figure 1.3) returned that all plants experienced the same level of growth stress- or lack thereof. Carbon isotope discrimination is a robust method commonly used to identify differences in water stress in plants. It has repeatedly been shown to have a significant increase during stressful conditions, specifically when water is limited i.e., drought (Vantghem, et al., 2021; Seibt, et al., 2008; Munjoji & Ayisi, 2021; Bhaskara et al., 2022;). Based on this physiological measurement, this allowed us to conclude that all of our plants were under identical growth conditions.

Due to the nature of our investigation into stomata, we also had to ensure the leaves among all our individuals were comparable. Previous literature indicates high variability in leaf stomata characteristics among subspecies, within a single plant, and

even throughout a single leaf (Bímová, 1992; Kubínová, 1994). We controlled for leaf maturity based on position in relation to the shoot apical meristem of each seedling. Based on leaf area measurements, there were differences at the population level (Figure 1.4). We chose to take data on a section of the leaf as opposed to the entire leaf area in order to control for larger leaves having different larger areas.

To control for the possibility that different areas of the leaf could have different stomata characteristics, we chose to image three areas of equal dimensions positioned lengthwise and not overlapping along the leaves, treating each as an independent unit for analysis, avoiding areas that could influence stomata development such as the leaf edges and epidermis directly superior to venation. This sampling protocol is modeled after the random selection outlined by Kubínová (1994) for leaf sampling when these specific development traits are unknown. We also confirmed that adaxial and abaxial surfaces did not significantly differ in stomata characteristics when all populations are aggregated (Figure 1.5). Based on our identically grown individuals and leaf sampling, we were confident that our data was robust for population level analysis.

Differences in stomata characteristics

After confirming that our seedlings were comparable at the population level, we distinguished differences in both stomata density and size among populations (Figure 1.6). This variation in greenhouse common garden seedlings suggests that our seedlings display fixed phenotypic traits and not plasticity. Our plants have retained traits from their original sample location as opposed to displaying the same phenotype that would be advantageous in the greenhouse conditions without water or drought stress. This conclusion is based on the nature of common garden experiments utilizing sampling of

wild populations all grown in identical conditions (de Villedenreuil et al., 2016). Fixed phenotypic traits would remain the same in the wild and in the greenhouse. This has been repeated for many species such as a similar experiment with *Arabidopsis lyrata* which confirmed local adaptation along latitudinal lines as well as in relation to drought (Paccard et al., 2014). Although we provide evidence that phenotypic plasticity is not responsible for these specific phenotypic traits, there are still other possibilities within the realm of genetics that could affect their expression. These phenotypic traits could be the direct result of a single gene, multiple genes, or epigenetics. Further analysis is needed to find the genetic underpinning of these phenotypic traits such as the methodology in the rabbitbrush study by Faske et al. (2021) which combined geographic, climatic, phenotypic, and genomic analyses to investigate local adaptation.

At the population level, we observed significant differences in stomata density and these differences conflict with our predictions (Figure 1.6A). Seedlings sampled from population UTT2 had on average the highest stomata density. This translates to the least efficient stomata existing in the most stressful drought environment. Seedlings from population IDT3 experiencing the lowest PET had the least dense stomata. We predicted the opposite based on literature suggesting that less density would be the most adaptive to drought conditions as it would maximize gas exchange and minimize excess water lost to transpiration (Meng, 2018; Bertolino et al., 2019; Gupta et al., 2020; Franks et al., 2015; Faralli et al., 2019). This indicates a more complex relationship between drought stress and stomata in sagebrush, possibly due to growth season time limitation as was observed with *Arabidopsis thaliana* populations that displayed higher WUE due to lower stomata

density in relation to their shorter growing season compared to other populations (Dittberner et al., 2018).

We also observed significant differences in stomata size (Figure 1.6B). Our predictions were partially correct, as UTT2 had on average, the smallest stomata. However, those seedlings' stomata were similar in size to ones from population IDT3, on the opposite side of our PET gradient. Across our PET gradient, a trend of more adaptive traits in more stressful conditions did not occur. A smaller size in stomata has been theoretically and empirically shown to increase WUE by reducing the amount of water lost through a faster kinetic response to drought (Paccard et al., 2014; Faralli et al., 2019).

Our methodology was primarily concerned with the relationship between local drought intensity based on water needs and stomata phenotype characteristics. There are other factors that could play a role such as the seasonal timing and duration of drought among our local climates (McDowell et al., 2008). Although our UTT2 population experienced the highest level of PET indicating higher water limitation, water resources in the area are affected by the North American monsoon. The North American monsoon occurs in a large area of North America with large storms fueled by ocean evaporation due to high heat in the summer months (Adams & Comrie, 1997; Boos & Pascale, 2021). The state of Utah lies in the northern portion of monsoon affected areas, translating to a shorter, albeit more intense, drought season for seedlings. More dense stomata could lose more water due to transpiration, but these plants do not have to conserve water for as long as ones in Idaho and Nevada. In *Arabidopsis lyrata*, local adaptation to seasonal drought length was correlated to WUE adaptations in stomata, however, these temporal factors were not the focus of this specific experiment and would prove difficult based on

a lack of higher resolution climatic data for all populations involved in our common garden (Paccard et al., 2014).

Differences in xylem diameter allocation

Taproot cross sections just below the crown of our seedlings allowed us to observe the earliest development of permanent vascular tissue. All of our seedlings showed multiple sections of vascular cambium tissue, consistent with the timeline of growth for our experiment. A multitude of shapes were observed, especially in the secondary xylem tissue, in part due to the presence of concavities in all of our seedlings (Figure 1.8), potentially creating individual effects that could skew comparisons among populations. In response, we measured the total area encompassed by the endodermis in each cross section and found no statistically significant differences at the population level (Figure 1.7), allowing us to continue measure xylem diameter allocation in the same fashion as McElrone et al. (2004).

Xylem vessels are a critical component in desert plants, maintaining a water column that is continuously being consumed by photosynthetic demands but cannot be replenished during periods of drought. Reducing xylem diameter translates to minimizing the risk of embolism, a trait variation observed in many woody plant species (Comas et al., 2013). We observed variation in the allocation of vessels at specific diameter classes of our seedlings at the population level (Figure 1.9). Population IDT3 had the greatest allocation of large diameter vessels, possibly due to the less stressful drought compared to the other populations conferring less risk of having these types of vessels. This is in line with our predictions and hypothesis that the most stressful environment poses the greatest risk of embolism, selecting seedlings with smaller diameter vessels to minimize

this risk. Smaller diameter vessels translate to smaller roots overall, which increases a plant's ability to acquire and retain water (Comas et al., 2013). The same trend of resistance to embolism following a gradient of drought stress was also seen in populations of European beech trees, with marginal populations exposed to higher temperatures and increased aridity having greater resistance to embolism (Stojnić et al., 2018).

Vascular tissue abnormalities

Previous work identified abnormal stem development in *Artemisia tridentata* and described it in detail in our specific study subspecies, *Artemisia tridentata* ssp. *tridentata* (Evans et al., 2019; Evans & Graney, 2018). We had the unique opportunity to observe and quantify the same abnormalities in well-watered seedlings grown in an identical common garden experiment, in contrast to the drought stress experienced by natural populations. Vascular tissue abnormalities are thought to be an adaptation of many desert species around the world to protect against whole plant cavitation under limited precipitation; when xylem vessels are disconnected into independent segments, one can fail due to embolism while the rest maintain their water pressure gradient (Schenk, 1999; Schenk et al., 2008). However, *all* of our seedlings had some form of damage to their vascular cambium, suggesting these abnormalities are adaptive traits and not a result of tissue damage due to aridity. Interestingly, we saw a similar amount of tissue loss in the stem area across our populations, with no trend with respect to PET.

Further Work

Our work has identified evidence for local adaptation in populations of basin sagebrush. The presence of variation in our common garden experiment attributes

genetics as underpinnings to differences phenotypic traits as opposed to phenotypic plasticity. However, the complex relationship we observed requires a more detailed approach to tease apart further climatic variables that could be driving selection of stomata characteristics. Across all of our sampled populations, individuals with low stomata density and small stomata size exist, conferring higher WUE and faster kinetic response to drought stress. However, there was no clear population which exhibited the most adaptive traits consistently. Population IDT3 had stomata conferring high WUE, but its xylem vessels confer higher risk of embolism. As a plant drought strategy, seedlings from IDT3 might develop stomata to minimize its transpiration loss over a longer period of time as a preemptive measure, prolonging its timespan with adequate water thereby negating the need to minimize risk of embolism. However, with increasing incidence and duration of drought stress due to climate change, this would leave it more vulnerable to death by vessel cavitation compared to populations with smaller vessels such as seedlings from UTT2. Seedlings from UTT2 have vessels conferring lower risk of embolism, but this would hinder its uptake of water during monsoon season, leading to decreased rate of growth, as larger vessels like those in seedlings from IDT3 would be able to carry larger amounts of water from its roots to its leaves.

These inferences paint an unclear picture for conservation and restoration efforts that might look for a superior line of sagebrush that maximizes both stomata and xylem phenotypes against drought. The existence of variation is a promising sign for the potential of these populations to adapt; with enough time, drought stress could cause selection for smaller and less dense stomata. Unfortunately, that kind of change necessitates a time scale an order of magnitude greater than quickly approaching drought

predicted by climate change research. Without signs of phenotypic plasticity, these populations are unable to supplement their resistance to drought in the meantime.

Although it paints a worrying assessment of adaptive capacity, this experiment only tested four populations from a much larger range which historically spanned over a third of North America. Future work with greater financial and logistical ceilings should sample more populations across more geographic and climatic clines. Methods such as a gene by environment experiment could confirm if phenotypic traits conferring greater drought tolerance occur during stressful environments. With the recent release of a reference quality genome for *Artemisia tridentata*, it is imperative to contribute to the genetic portion of genome to phenome research on sagebrush, possibly with whole genome sequencing to look for genetic variation that could directly explain phenotypic variation. Linking phenotyping and genotyping work as already proven successful in investigating adaptive traits against drought in many species such as rubber rabbitbrush, another important shrub in Western North America (Faske et al., 2021). Hopefully, genome to phenome research will provide the tools necessary to adequately save sagebrush populations and the sagebrush steppe as a whole, a unique and important ecosystem in our own backyards.

CHAPTER TWO: DETERMINING GENETIC UNDERPINNING OF PHENOTYPIC
DIFFERENCES OBSERVED FROM A STUDY OF SAGEBRUSH SEEDLINGS

Abstract

To combat species losses due to climate change, population vulnerabilities must be quantified with respect to their potential to respond based on their genetic variability allowing adaptation. A phenotype study identified significant differences sagebrush seedling traits related to water use. We hypothesized that due to differences in local climate, populations have undergone local adaptation. We predicted differences in genomes would cluster individuals similar to previous climatic and phenotypic analyses. We chose 12 total seedlings representing three populations occurring along a climatic gradient for genome re-sequencing. Reads were trimmed, cleaned, and mapped to the *Artemisia tridentata* ssp. *tridentata* pseudo-chromosome reference genome. Variants were called and extensively filtered resulting in a dataset of 23,330 single nucleotide polymorphisms (SNPs). Our analysis returned a top eigenvector explaining ~15% variance that segregated our 12 samples into two groups, consistent with phenotypic and climatic analyses. This supports the hypothesis that populations of sagebrush evolved phenotypes that are locally adapted and genetically controlled, not under phenotypic plasticity. These populations, if given enough time on an evolutionary scale, have the potential to select for more adaptive traits to combat climate change. Future research should look at specific populations rich in gene variants conferring increased water use efficiency.

Introduction

Genomics in the Age of Climate Change

Human driven climate change is projected to have drastic impacts for ecosystems and biodiversity around the world in the very near future (Xu et al., 2018; IPCC 2022). Restoration and conservation plans aimed at reducing these impacts must be informed by genetic research measuring species potential to adapt and overcome these impactful climate consequences, maximizing our resources (IPCC 2022; Ofori et al., 2017). Ideally, plant populations would already have adaptations to more severe drought and heat underpinned by heritable genes. However, most plants have evolved to thrive in historical conditions unsuited for extreme climate events such as the intense megadrought in North America (Stahle, 2020; Williams et al., 2020). More realistically, some members of populations might exist that exhibit phenotypic traits that allow greater chance of survival compared to the average individual. If genetically controlled, these traits can be passed down to subsequent generations and a population can adapt to new climate conditions at the rate of evolutionary fixation of the adaptive phenotypic traits. This process has been observed in some plant populations in the American Southwest; in the past few decades, populations of shrubs and trees have, in the presence of severe drought, increased in intrinsic water use efficiency (iWUE) a ratio of a plant's photosynthetic yield to their water loss indicative of drought response and tolerance (Kannenberget al., 2021). Over time, adaptive traits will be the dominant alleles in the population- this defines evolutionary adaptation. If the adaptive capacity of a population does not sufficiently overcome the extremes of climate change, human intervention can transplant adapted plants to supplement populations, restoring ecosystem health. To measure a species'

potential to adapt it is important to find standing variation in heritable phenotypic traits (Aitken et al., 2008; Ofori et al., 2017). Researchers have repeatedly taken advantage of local adaptation following clines and gradients in local climates or geographies as a source of heritable phenotypic variation (Franks & Hoffman, 2012).

Tapping into Local Adaptation

Phenotypic variation underpinned by genetics due to local adaptation has been investigated in several plants such as Arabidopsis, barley, corn, and poplar (Dittberner et al., 2018; Chen et al., 2019; Dunn et al., 2019; Hughes et al., 2017; Oladosu et al., 2019; Arango-Velez et al., 2011; Rumman et al., 2017). Many researchers in the past measured phenotypes of plants grown in reciprocal transplant experiments, looking at varying levels of fitness in translocated samples across different common gardens (Savolainen et al., 2013). Similarly, greenhouse common garden experiments using uniform growth conditions have been used to find relationships between phenotypic variation and geographic variation without needing multiple growing locations (Pazourek 1973; Aitken et al., 2008). These well-established methodologies look for signs of local adaptation but cannot discern the role of epigenetic mechanisms. However, when coupled with modern genotype-by-sequencing approaches, we can look at the genetic underpinnings of traits. If observed genetic variation matches variation in phenotypes, then genetic control for traits is the probable cause (Aitken et al., 2008; de Villemereuil et al., 2016). Epigenetic mechanisms affect phenotypic trait expression without changing DNA. A signal of epigenetic mechanisms will be evident if populations exhibit phenotypic variation without genetic variation to support these observations (Franks & Hoffman, 2012). By utilizing a genome to phenome to find variation and understand where it originates,

population adaptive capacity can be quantified to inform predictions into how they will face climate change. One ecosystem with such vulnerable populations is the sagebrush steppe in Western North America, built up by its widespread keystone species big sagebrush.

Summary of Previous Phenotypic Research

The keystone species of the sagebrush steppe, big sagebrush- *Artemisia tridentata*-, is under threat by many factors including human land use change, wildfires, and drought all exacerbated by anthropogenic climate warming (Xu et al., 2018; Coop et al., 2020; Stahle, 2020; Williams et al., 2020). A previous common garden experiment grew sagebrush seedlings (*Artemisia tridentata* ssp. *tridentata*) sampled from locations with different climates representing a gradient of potential evapotranspiration (PET). The experiment found significant differences in phenotypes associated to water use in a plant already adapted to tolerate drought. Leaf stomata and xylem characteristics were measured after two years, showing significant variation in stomata density and size as well as xylem diameter allocation, pointing to signs of local adaptation associated to their respective local climates.

The findings of that phenotyping study decrease the likelihood that plasticity is involved due to how the seedlings, on average, retained individual population characteristics as opposed to showing little variation as a response to maximizing the lack of water deficit in the greenhouse conditions. We can investigate the different possibilities of what causes phenotypic variation by leveraging the benefits of a common garden experiment by sequencing and looking for variation in their genomes. Understanding the genetics of these threatened populations will inform our understanding

of their adaptive capacity, a key tool to improve conservation and restoration of an important keystone species (Chaney et al., 2017).

Objectives & Hypotheses

Our main objective for this experiment was to explore the genomic underpinnings of phenotypic differences between populations of sagebrush sampled from different local climates. We sought to look at signs of genetic differentiation by assembling genomes and looking mutations, specifically, single nucleotide polymorphisms (SNPs). A newly published reference quality genome for *Artemisia tridentata* ssp. *tridentata* was utilized for this work.

The first objective was to make chromosome level comparisons of genomes across populations of diploid basin sagebrush. The first genome assembly for *Artemisia tridentata* observed high levels of complexity and heterozygosity with evidence of previous polyploidization and diploidization (Melton et al., 2022). We hypothesized that our sampled individuals all share the same complex evolutionary history and share homology among chromosomes. This would allow us to compare their mutations and variation among reassembled genomes. Our second objective was to investigate if phenotypic variation observed in chapter one of this thesis is underpinned by genomics and not epigenomics. We predicted that an analysis using dataset of genetic variants should cluster our samples in the same fashion as previous climatic niche and phenotype principal components analyses (PCA). Seedlings from IDT3 and NVW1 originating from locations with lower PET and exhibiting less dense stomata should be clustered separately from seedlings from population UTT2 with experiencing higher PET and exhibiting more dense stomata.

Methods

Sampling

Based on phenotype analyses of seedlings grown from a common garden greenhouse experiment, I chose to sample four individuals each from populations IDT3, NVW1, and UTT2. These seedlings were sampled from locations with different climates, grown in identical optimum conditions, and displayed phenotypic variation consistent with genetic control of phenotypes. Each population, on average, displayed a unique combination of stomata characteristics (density and size) based on statistically significant pairwise contrasts at the population level.

DNA Extraction & Resequencing

DNA extraction was conducted on 12 seedlings in March 2022 using the QIAGEN DNeasy Plant mini kit (Hilden, Germany; catalogue # 69204) using approximately 20 mg of plant leaf tissue per sample. These seedlings were originally preserved for herbarium storage in July of 2021. The 12 samples were processed for library preparation and Illumina HiSeq (San Diego, CA, USA) whole genome paired-end sequencing (2 × 150 bp; ~20x read depth) by Azenta Life Sciences (New Jersey, NJ, USA), formerly Genewiz Inc.

Bioinformatics

Raw reads were checked for quality using FastQC (Andrews, 2010; <https://www.bioinformatics.babraham.ac.uk/index.html>). Trimming of reads was done using Trimmomatic v.0.36 (Bolger et al., 2014). Raw reads were trimmed and cleaned with a low percentage of loss- on average 1.03% (Table 2.3). Trimmed reads were aligned and mapped to the reference genome of *Artemisia tridentata* ssp. *tridentata*

(GenBank Accession: JAKJXK000000000) using DNA alignment software ‘Bowtie 2’ (Langmead & Salzberg, 2012). Software ‘minimap2’ was used to map consensus sample sequences to the reference genome to generate ‘PAF’ files for chromosome analysis.

Variants were called using software ‘bcftools’ (available at: <http://samtools.github.io/bcftools/>) and manipulated in R using package ‘vcfR’ (Knaus & Grunwald, 2017). We used a dataset unique pipeline for filtering based on read quality higher than 30 due in part to our low sample number, read depth above our mean of 7 due to the species history of polyploidization and subsequent diploidization, missingness threshold at 0.2, minor allele frequency threshold of 0.05, and mapping quality higher than 20 due to genome complexity. This was accomplished using built-in ‘bcftools’ filtering criterion. The filtered dataset of SNPs was then pruned with a linkage disequilibrium threshold of 0.2 using R package ‘SNPRelate’ (Zheng et al., 2012).

Analyses

Utilizing generated ‘PAF’ files, chromosome comparison analyses were conducted. Dot plots were generated using R packaged ‘dotPlotly’ (<https://github.com/tpoorten/dotPlotly> accessed on 1 June 2022) to look for chromosomal rearrangements and genome similarity between each of our samples and the reference genome. Genome coverage maps were generated using R package ‘pafr’ to assess coverage against the reference and again visualize any large structural rearrangements. Heatmaps of chromosomal similarities were generated using R to visualize percent similarities comparing each sample chromosome to the reference.

We investigated genetic variation in our SNPs dataset with a principal component analysis (PCA) at the individual level using R package ‘SNPRelate’ (Zheng et al., 2012).

To further look at genetic differentiation and add statistical support to the power of our sampling, a bootstrap analysis run at 1000 iterations was utilized to create a dendrogram based on genetic differentiation using R package ‘poppr’ (Kamvar, Brooks, & Grunwald, 2015).

Further analysis on our dataset was done as a preliminary exploration of population genomics of sagebrush. We tested Hardy-Weinberg Equilibrium at every locus using R package ‘pegas’ (Paradis et al., 2010). Levels of heterozygosity were tested at the population level using R package ‘vcfR’ (Knaus & Grunwald, 2017). A STRUCTURE analysis investigating ancestral population structure of our three populations was conducted using R package ‘LEA’ (Frichot, 2015). STRUCTURE analysis was run with $K = 1:15$, at 10 repetitions, over 10,000 iterations.

Results

Sampling for DNA Extraction

All individuals from populations IDT3, NVW1, and UTT2 were plotted based on stomata density and size. This visualized which seedlings most exemplified the average stomata characteristic types for each population based on how far into their respective phenotype quadrant each seedling occurred in. Four individuals from each population, most in line with their characteristic stomata type, were chosen for DNA extraction (Table 2.1).

Genomic Dataset

All 12 samples were sequenced producing a raw dataset of 3,091,460,681 paired end reads returned with a mean quality score of 35.59 (Table 2.2). Average raw genome coverage was estimated at 18x. Reads were cleaned and trimmed with an average drop rate of 1.02% (Table 2.3). The total number of biallelic SNPs generated for our dataset after our quality filtering procedure was ~13 million. This dataset was then pruned at a linkage disequilibrium threshold of 0.2, resulting in a final set of SNPs for analysis totaling 23,330. This final data set is what was used to further analyses of genetic variation.

Analyses

All chromosome level analyses returned high levels of similarity between our twelve samples and the reference genome. No large chromosomal abnormalities were found (Figure 2.1 & 2.2). With a sliding window one million base pairs in size, we found genome differentiation when compared to the reference genome to be less than 1% (Figure 2.3).

A principal component analysis (PCA) returned a top eigenvector with ~15% explained variance, separating our 12 samples into two clusters mirroring the phenotypic clustering separating population UTT2 from populations IDT3 and NVW1 in previous climatic niche analyses (Figure 2.4). A dendrogram based on genetic differentiation returned a bootstrap support value of 100 for the same clustering pattern at the population level as our PCA (Figure 2.5).

Preliminary population genomics analyses were done to explore meta-population structure but did not yield conclusive results due to our insufficient sampling size. An

analysis of Hardy-Weinberg equilibrium across all loci with variants indicated a large majority of loci not in equilibrium. We also found high levels of heterozygosity at the individual level (Table 2.4), consistent with findings by Melton et al. (2022). A STRUCTURE analysis investigating the likely number of ancestral populations returned a cross-entropy plot (Figure 2.6) denoting a single ancestral population as the best hypothesis. The next two values of K which had slightly higher entropy loss were $K = 2$ and $K = 14$ (Figure 2.7), with the former partitioning our samples into the same population structure in line with previous genetic, climatic, and phenotypic clustering, while the latter showed no population level distinctions indicative of previous gene flow across all three locations. Each individual displayed a level of heterozygosity above 0.10 (Table 2.4).

Discussion

Genomic Data

The consequences of climate change require an understanding of how they threaten populations of vulnerable species and the capacity of populations to adapt and respond to them. This capacity is rooted in how existing heritable variation in phenotypic traits generates potential for evolutionary adaptation to occur. Previous phenotypic variation was observed in populations of a keystone sagebrush species experiencing different local climates. After assembling genomes of sampled individuals using a reference-based approach, genomic variation provides evidence for genomic underpinning for phenotypic variation.

Basing genomic analysis on phenotypic variation

The twelve individuals sampled for re-sequencing (Table 2.1) were deliberately chosen to represent the average population stomata characteristics found to be statistically significant. Population IDT3 had lower stomata density and smaller stomata size. Population NVW1 had similarly lower stomata density but larger stomata size. Population UTT2 had the highest stomata density but smaller stomata size. There were individuals in each population that did not exemplify these average characteristics, and these were avoided for re-sequencing in order to maximize any genomic signal. Although this methodology was not random, this was the most effective due to sampling and cost limitations. Genetic analysis did not include individuals from population IDT1, although individuals were available from the previous common garden experiment. This population was also grown in the same common garden greenhouse experiment but did not display statistically significant pairwise contrasts when compared to other populations, making further genetic comparisons at the population level less clear. It is a known site of restoration supplemented with individuals originating from Utah, an origin location with a different climate with the potential to impact investigations into population structure, gene flow, and local adaptation.

Genome Comparisons

Before looking at small scale differences in our specimens' genomes, we first investigated their overall chromosomal structure to see if they were comparable. All of our re-sequenced individuals displayed genomes highly similar in structure to the published reference genome for *Artemisia tridentata*, mapping onto the nine pseudo-chromosomes. This was important to verify due to the complex history of sagebrush

polyploidization, diploidization, and hybridization (Melton et al., 2022). Dot plots showed a direct alignment between the reference genome and all 12 of our individuals, as observed by a straight, unbroken line in all plots (Figure 2.1), absent of any scattered points that signal deviance commonly seen on dot plots. Genome coverage maps also showed direct mapping between the reference genome and all 12 individuals, as each chromosome was identified solely by one color, indicating no rearrangements (Figure 2.2). We generated a heatmap comparing our samples at the chromosome level to the reference genome. It displayed divergence of less than one percent for all chromosomes (Figure 2.3). Interestingly, the heatmap did not group our samples within population clusters. Two major clusters were returned with one mixing seedlings from IDT3 and NVW1, while the other included seedlings from all three populations. We attributed this to the relatively large viewing window utilized by the ‘minimap2’ software affording lower resolution when comparing highly similar sequences. A test for meta-population structure could test if gene flow among populations could add evidence to this clustering model, but that would be beyond the scope of this study. Across our chromosome level comparison, our results gave us confidence to generate a dataset of single nucleotide polymorphisms (SNPs) for analyses of genomic variants.

Genome underpins phenome

Knowing we have homologous chromosomes to compare, we then searched for SNPs and ran variants through an extensive filtering process. A preliminary dataset using filtering similar to commonly used population genomics methodology yielded dataset with relatively low explained variance. We suspected this to be due to the nature of the sagebrush genome, one that is highly heterozygous and high in repeats (Melton et al.,

2022). In response, we used additional filtering parameters including an increased base PHRED quality score of 30, data specific read depth, and mapping quality to ensure our dataset contained appropriately mapped biallelic SNPs *only*. Highly repetitive regions pose a problem for computational bioinformatics, a primary concern for our pipeline as the reference genome is made of 77.99% repeat sequences (Melton et al., 2022). For our specific dataset, our haploid base coverage was $k = 7$. For our dataset, SNPs that were mapped to a read depth of 14 would represent homozygous alleles on our reassembly. Any of our SNPs that were mapped with values greater than 14 could be seen as signals of polyploidy, or more likely a SNP that exists in one locus on the genome but was mapped to a similarly repetitive locus somewhere else betraying the biallelic assumption for that SNP. These were trimmed along with low *mapping* quality variants. We also did not filter for only neutral variants, instead combining adaptive and neutral variants together for analysis. Our phenotypes in focus are ones that confer gains in fitness and assumed to be under selection, therefore looking at only neutral SNPs would not yield appropriate results.

Based on a PCA (Figure 2.4), the top eigenvector clustered our individuals in the same fashion as previous climate and phenotype analyses, with individuals from IDT3 and NVW1 closer together, separated from individuals from UTT2 (see Chapter 1). We can now correlate previously observed phenotypic differences to genetic differences, pointing to local adaptation based on local climate (Elfarargi et al., 2023). Due to our low sampling, we utilized a bootstrap analysis to generate a dendrogram to infer the statistical power of our dataset. Our dendrogram returned high support to our population divisions. Seedlings from UTT2 are genetically different from seedlings from IDT3 and NVW1

supported by a bootstrap value of 100. The branching within the IDT3 and NVW1 division shows far lower support, indicating higher similarity, confirming predictions that their more similar climates would select for similar traits and genetics.

Peeking into population genomics

Due to cost limitations, we were unable to maximize our sampling by using all available greenhouse common garden plants for genetic analysis. The twelve individuals could not afford enough resolution to answer questions regarding population genetics, however, preliminary analyses were conducted to direct future research. A STRUCTURE analysis looking at meta-population structure returned a value of $k = 1$ as the yielding the lowest value of cross-entropy (Figure 2.6). Looking at our SNP dataset at the population level, we found high levels of heterozygosity (Table 2.4) and a majority of loci *not* in Hardy Weinberg Equilibrium. This is in line with our dataset having loci under selection. These results suggest one large metapopulation with signal of previous gene flow across large geographic area in the mountainous sagebrush steppe. The sagebrush steppe was historically a large homogenous landscape, but populations are fragmenting at an alarming rate due to many factors such as climate warming and human land use change. Our preliminary populations genomics results might indicate that these fragmented populations are still actively evolving as gene flow has only recently been cut off. These are hypotheses that need to be tested, as large population genomics inquiries require larger sampling and a greater breadth of geographies and climates represented across the entirety of the sagebrush steppe's historical range.

Future Research

Our results suggest phenotypic differences are underpinned by genomics, paving the way for future studies looking at specific genes that could improve survival of sagebrush seedlings in drought. Various genes have already been implicated in stomata development and function such as: *EPF1*, *MPK12*, *BAK*, *OST1*, *SLAC1*, *SYP121* (Wang et al., 2012; Hughes et al., 2017; Dunn et al., 2019; Eisenach et al., 2012). Sagebrush has a larger genome than its relatives with lots of potential homologs and replicates of these genes. A draft genome study identified an enrichment in aquaporin genes (AQPs) which could be a result of adaptation to the arid climate of Western North America (Melton et al., 2021). Studies into specific SNP mutations in replicated homologous genes that change stomata characteristics could give insight into the mechanisms that lead to WUE differences among populations. Similarly, a genome wide association study (GWAS) could identify important loci for stomatal phenotypes. However, a GWAS would require a larger sample representing more populations in the sagebrush steppe to yield reproducible and robust associations between phenotypes and loci (Uffelman et al., 2021). A larger sample size could also allow more genome to phenome work such as understanding the distribution of genetic variants along with a greater number of climatic variables for analysis. This approach was used previously in red spruce to qualify local adaptation in the context of climate and geography, identifying adaptive genes important to environmental tolerances (Casablanca et al., 2023).

In regard to the specific sagebrush lines utilized for this study, more experiments should be done looking at their response to stress. Our sampling included only well-watered seedlings from a greenhouse experiment. It must be seen if the same phenotypic response is seen when seedlings are grown with limited water, as environmental factors

have been known to affect stomata traits, as was seen in a reciprocal transplant experiment on *Thalictrum alpinum* (Zhang et al., 2012). Downstream regulation could play a role in affecting stomata development when under extreme stress. Drought sensitive genes such as kinases found by Chen et al. (2018) would be good candidates for RNA sequencing these same plants in a controlled drought experiment. Understanding that these genomes are very similar, how these genes are turned on and off in response to stress could inform the mechanisms that sagebrush utilize to tolerate drought.

The results of these experiments provide evidence that populations of sagebrush exhibit phenotypic trait variation in stomata and xylem that are underpinned by variation in their genomics. These phenotypes are key to how plants use water in order to improve drought tolerance. Due to their underpinning by genes, these traits are heritable, giving populations the potential to adapt, given enough time. However, this process might not be fast enough. Climate change occurs on a time scale far faster than slow-growing sagebrush. Instead, human intervention can supplement these populations with more individuals that have genes expressing traits more likely to confer drought tolerance. A targeted restoration utilizing well-adapted plant lines could overturn a history of repeated failures to recover the sagebrush populations lost to wildfires, land use change, and drought.

© 2023

Carlos Dave Contreras Dumaguit

ALL RIGHTS RESERVED

Carlos Dave Contreras Dumaguit

SOME RIGHTS RESERVED



This work is licensed under a Creative
Commons Attribution-Noncommercial
4.0 International License.

APPENDIX A



Figure A.1 Map of sagebrush populations 1

TABLES

Table 1.1 Sampled populations for greenhouse common garden.

Population	State	Coordinates (longitude, latitude)	Potential Evapotranspiration (PET)	Number of Seedlings Sampled for Leaf Phenotyping	Number of Seedlings Sampled for Root Phenotyping
IDT3	Idaho	-116.9641, 43.3366	1537	10	9
IDT1	Idaho	-115.657, 43.0962	1655	10	9
NVW1	Nevada	-117.7751, 41.5147	1767	10	8
UTT2	Utah	-109.3876, 38.306	1790	11	9

Table 2.1 Table of seedlings sampled for genome resequencing.

Seedling ID	Population	Average Stomata Density	Average Stomata Size
GH_0029	IDT3	73.06	28.92
GH_0143	IDT3	92.78	28.16
GH_0163	IDT3	103.06	27.33
GH_0192	IDT3	84.44	27.75
GH_0246	NVW1	83.61	29.78
GH_0326	NVW1	111.94	32.01
GH_0379	NVW1	63.06	30.33
GH_0399	NVW1	75.83	30.04
GH_0422	UTT2	143.61	29.13
GH_0443	UTT2	130.83	25.01
GH_0541	UTT2	214.44	28.64
GH_0579	UTT2	152.22	27.61

Table 2.2 Raw sequencing data statistics.

Sample_ID	Number of Reads	Yield (Mbases)	Raw Sequencing Coverage (x)
143	247166224	74150	17.66
246	275405858	82622	19.68
326	268168732	80451	19.16
541	261148484	78345	18.66
29	285199259	85560	20.38
192	197609615	59283	14.12
422	334891756	100467	23.93
579	246614832	73984	17.62
399	255482185	76645	18.26
443	230694350	69208	16.48
379	247397963	74219	17.68
163	241681423	72504	17.27

Table 2.3 Read trimming data statistics.

Sample_ID	Number of input read pairs	Number of reads both surviving	Number with only forward reads surviving	Number with only reverse reads surviving	Number of reads dropped	Percent of reads dropped
143	247166224	234457881	6511528	3827161	2369654	0.96
163	241681423	230281206	5621496	3858902	1919819	0.79
192	197609615	185985128	5640046	3430866	2553575	1.29
246	275405858	261152659	7522600	4274415	2456184	0.89
29	285199259	269674411	8132506	4526159	2866183	1.00
326	268168732	253558610	7497791	4162940	2949391	1.10
379	247397963	232641548	7985559	3565324	3205532	1.30
399	255482185	241492401	7150277	4089653	2749854	1.08
422	334891756	312301759	14310484	4736056	3543457	1.06
443	230694350	218701552	6152272	3605857	2234669	0.97
541	261148484	247255514	7318509	4037575	2536886	0.97
579	246614832	235354379	5754521	3364016	2141916	0.87

Table 2.4 Level of heterozygosity per individual

Population IDT3			
29	143	163	192
0.13773	0.12014	0.10941	0.1383

Population NVW1			
246	326	379	399
0.12282	0.12148	0.11083	0.1323
Population UTT2			
422	443	541	579
0.12023	0.112666	0.114721	0.120524

FIGURES

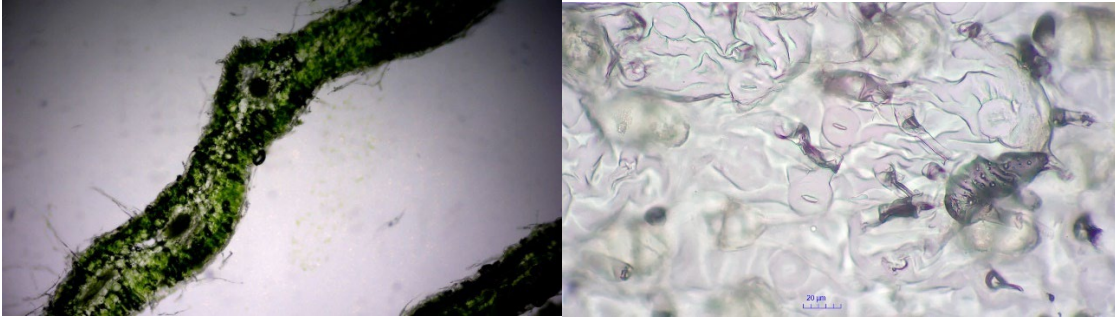


Figure 1.1 Microscopic images of sagebrush leaf (*Artemisia tridentata* ssp. *tridentata*). **LEFT.** Transverse cross section of a sagebrush leaf. Note the presence of green photosynthesizing palisade cells interior to both epidermis layers. Sagebrush leaves have an isobilateral amphistomatous structure, allowing for high conductance of CO₂ and shorter distance of gas diffusion utilizing stomata found on both surfaces. **RIGHT.** Image of leaf epidermis resulting from stomatal assay protocol. Taken at 400x magnification.

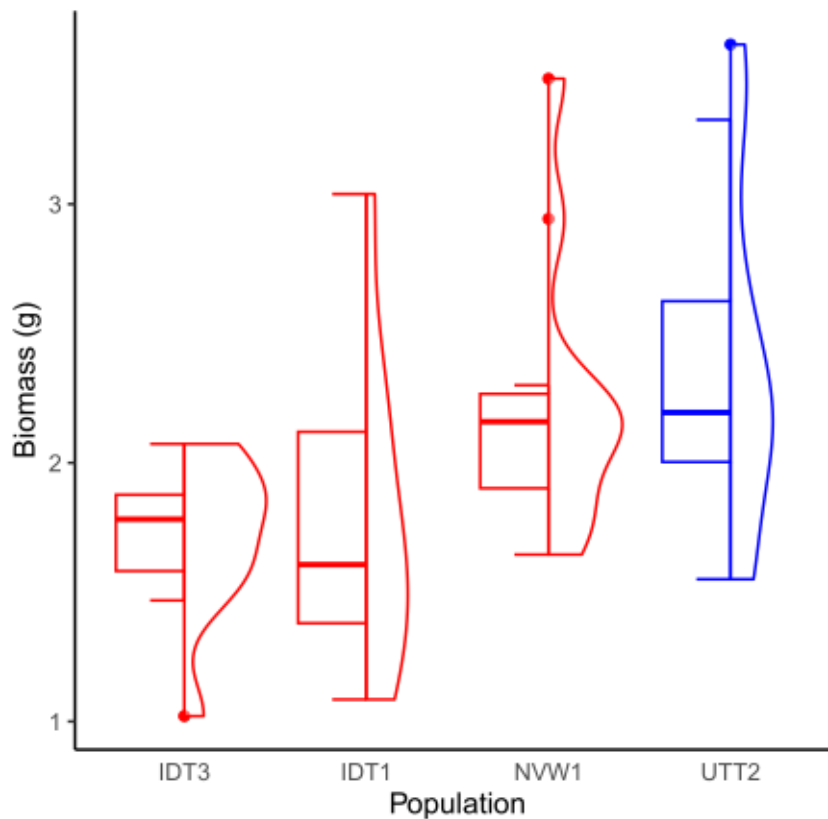


Figure 1.2 Half-violin-boxplot comparing biomass (grams) across populations of identically grown greenhouse sagebrush seedlings (*Artemisia tridentata* spp. *tridentata*). Populations are arranged in increasing PET value. Total plant biomass showed variation under identical optimum greenhouse conditions. A Kruskal-Wallis test returned a statistically significant effect of at least one population's distribution over the others (p-value < 2.2e-16). However, a post hoc Dunn's test looking at pairs of populations did not return any significant pairwise contrasts.

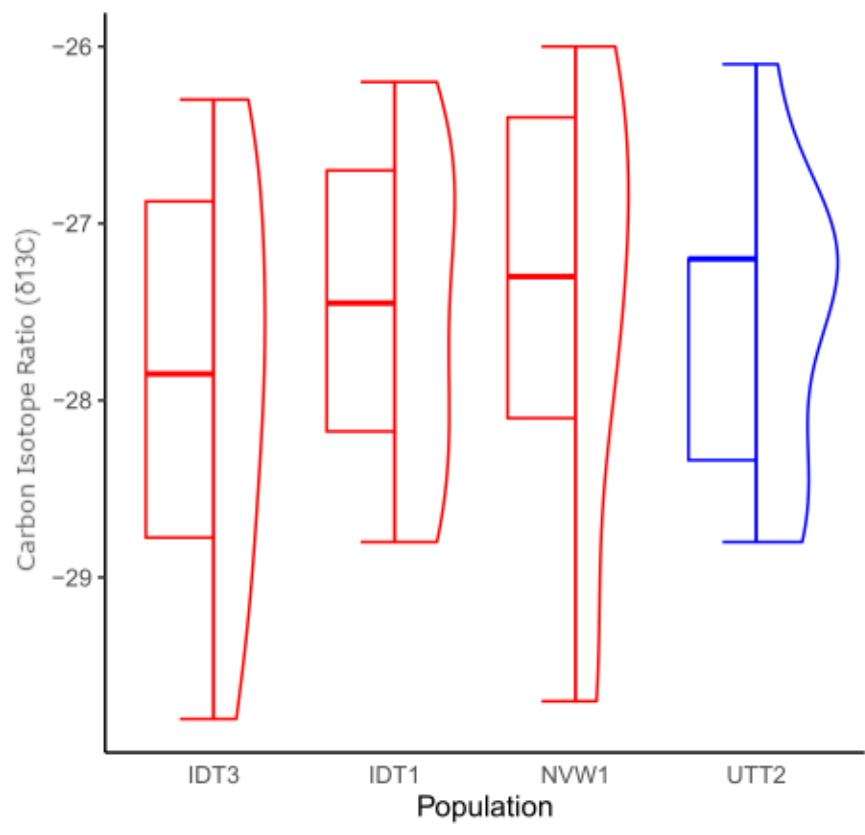


Figure 1.3 Half-violin-boxplots of carbon isotope ratios among identically grown greenhouse sagebrush seedlings. A GLM returned no statistically significant differences at the population level ($\alpha < 0.05$). From this, we can infer that the water use efficiency (WUE) of all our seedlings were similar, with all experiencing the same lack of water stress when combined with our well-watered conditions.

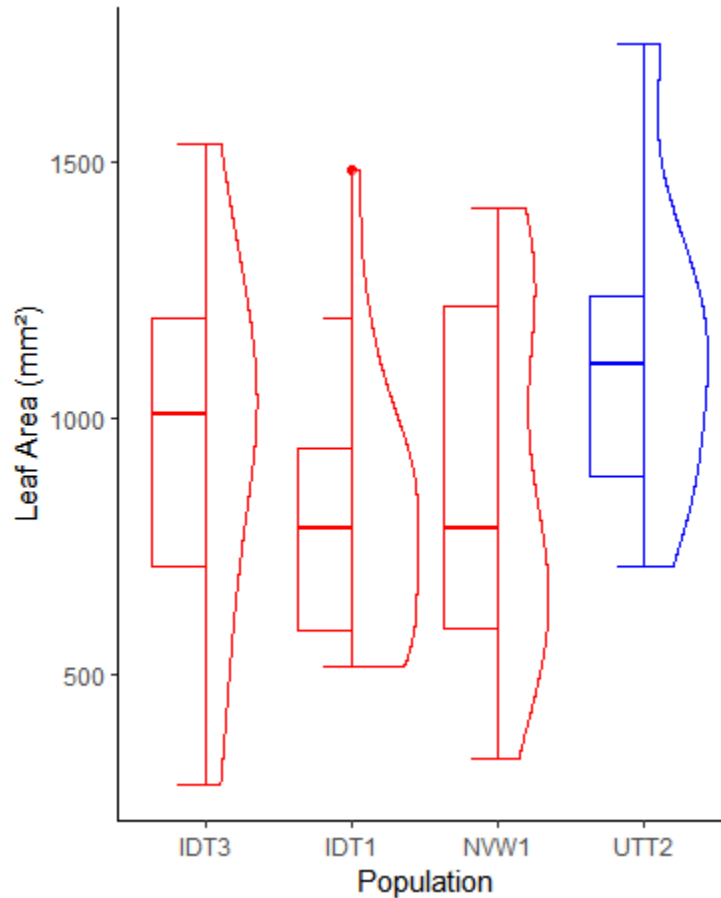


Figure 1.4 Boxplot of leaf areas from sampled sagebrush seedlings. A generalized linear model (GLM) returned a significant population effect (p-value = 0.0577; $\alpha < 0.05$).

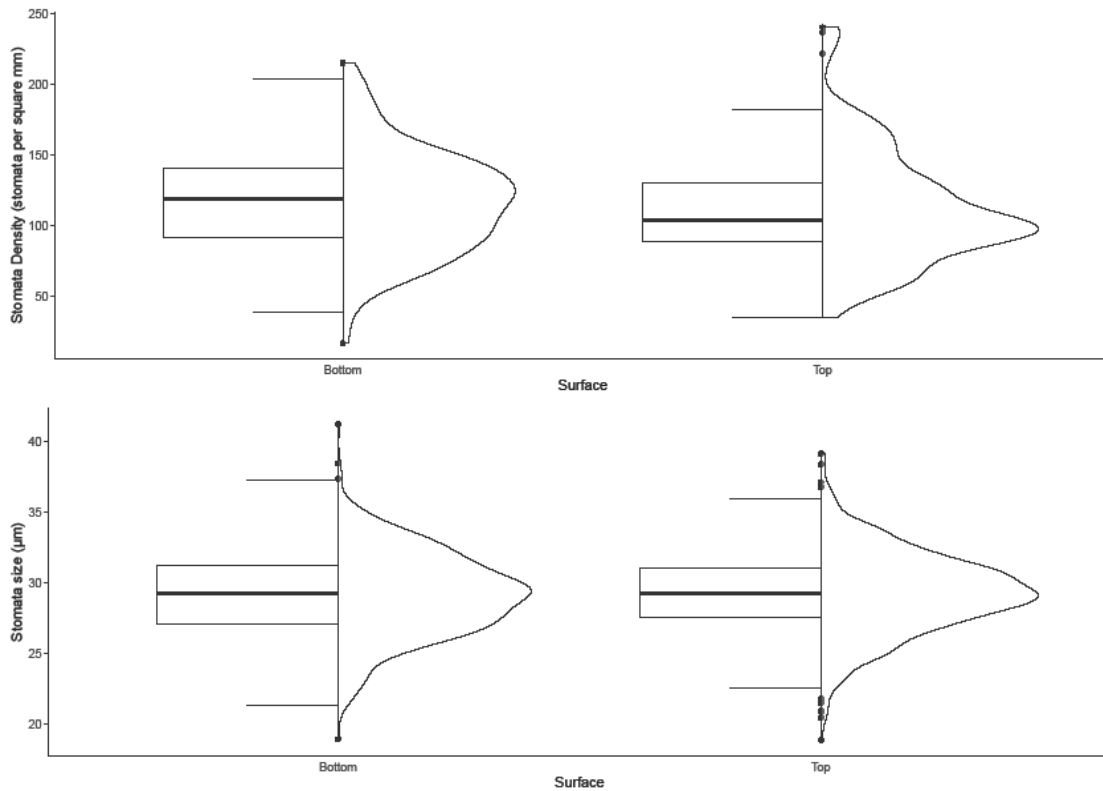


Figure 1.5 Half-violin-boxplot comparing stomata characteristics between adaxial (top) and abaxial (bottom) surfaces in sagebrush leaves. No statistically significant differences were found between leaf surfaces ($\alpha < 0.05$), allowing for downstream phenotype analysis. **A.** Two leaves were sampled from 41 plants, each representing data from one leaf surface. Three identically sized viewing windows (six per seedling) were counted for stomata density calculations. **B.** Four stomata were measured for every viewing window (24 per seedling) for stomata size calculations.

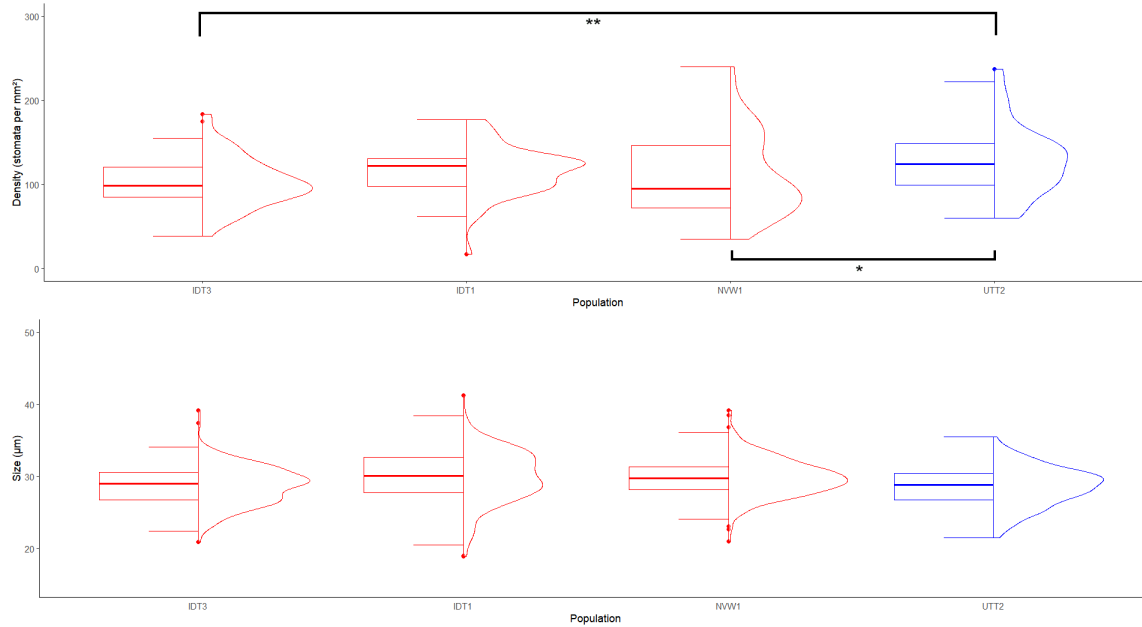


Figure 1.6 Half-violin-boxplot comparing stomata characteristics across sampled populations of sagebrush seedlings. RED denotes populations found within the ALPHA cluster (populations IDT3, IDT1, & NVW1) from a previous climatic principal component analysis (PCA) while BLUE denotes inclusion within the BETA cluster (population UTT2). A. Stomata density showed variation and statistically significant differences at the population level. B. Stomata size also showed variation and statistically significant differences at the population level.

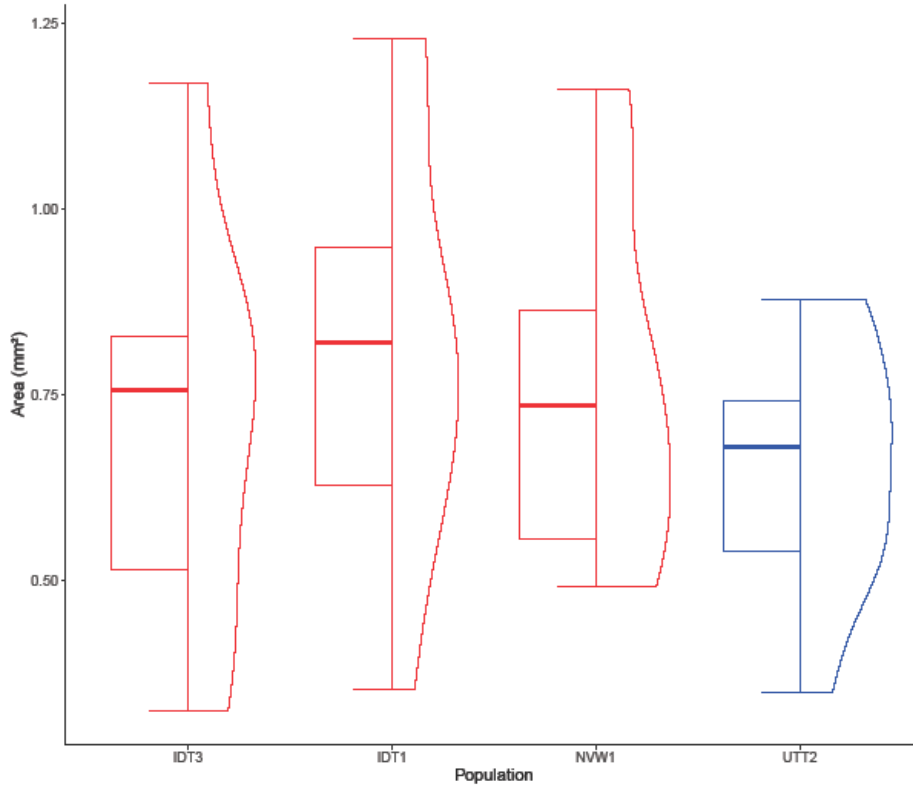


Figure 1.7 Half-violin-boxplot comparing area of encapsulated by the endoderm at the population level. Measurements were taken at the crown of each seedling, the widest and oldest area of vasculature. Seedlings' endoderm areas did not show any population effect, translating to similar amounts of transverse cross-sectional area of endoderm tissue across all populations.



Figure 1.8 Image of transverse cross-section of sagebrush seedling 0099. Note the presence of damage to the vascular cambium as outlined in red. These areas are void of vascular tissue, as opposed to being part of a continuous unbroken area in the shape of a circle. Larger light blue circles in the bottom of the image are xylem while the smaller richer blue circles that have taken dye are phloem cells.

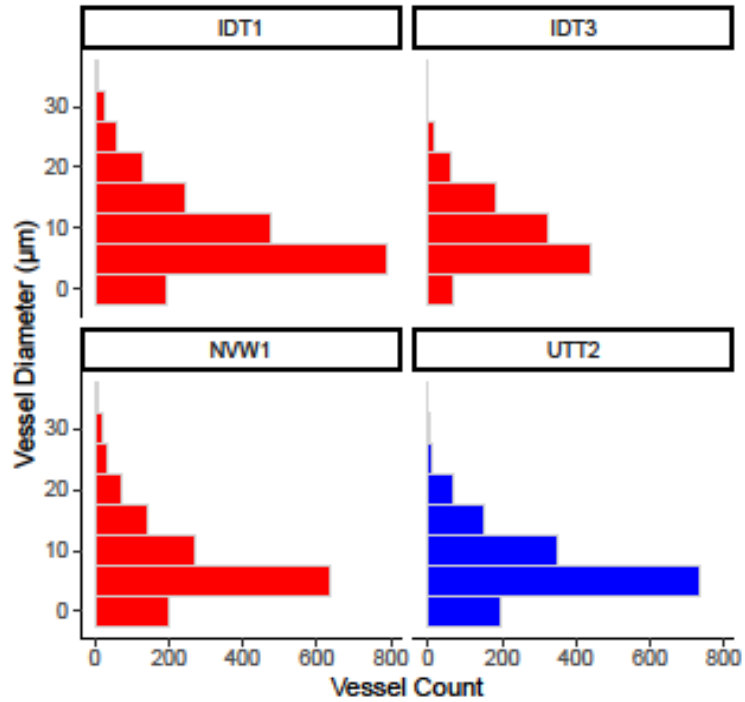


Figure 1.9 Bar plots of xylem allocation at diameter intervals across sampled sagebrush populations. Population IDT3 showed the largest percentage allocation to large diameter vessels compared to other populations, increasing risk of embolism during drought conditions.

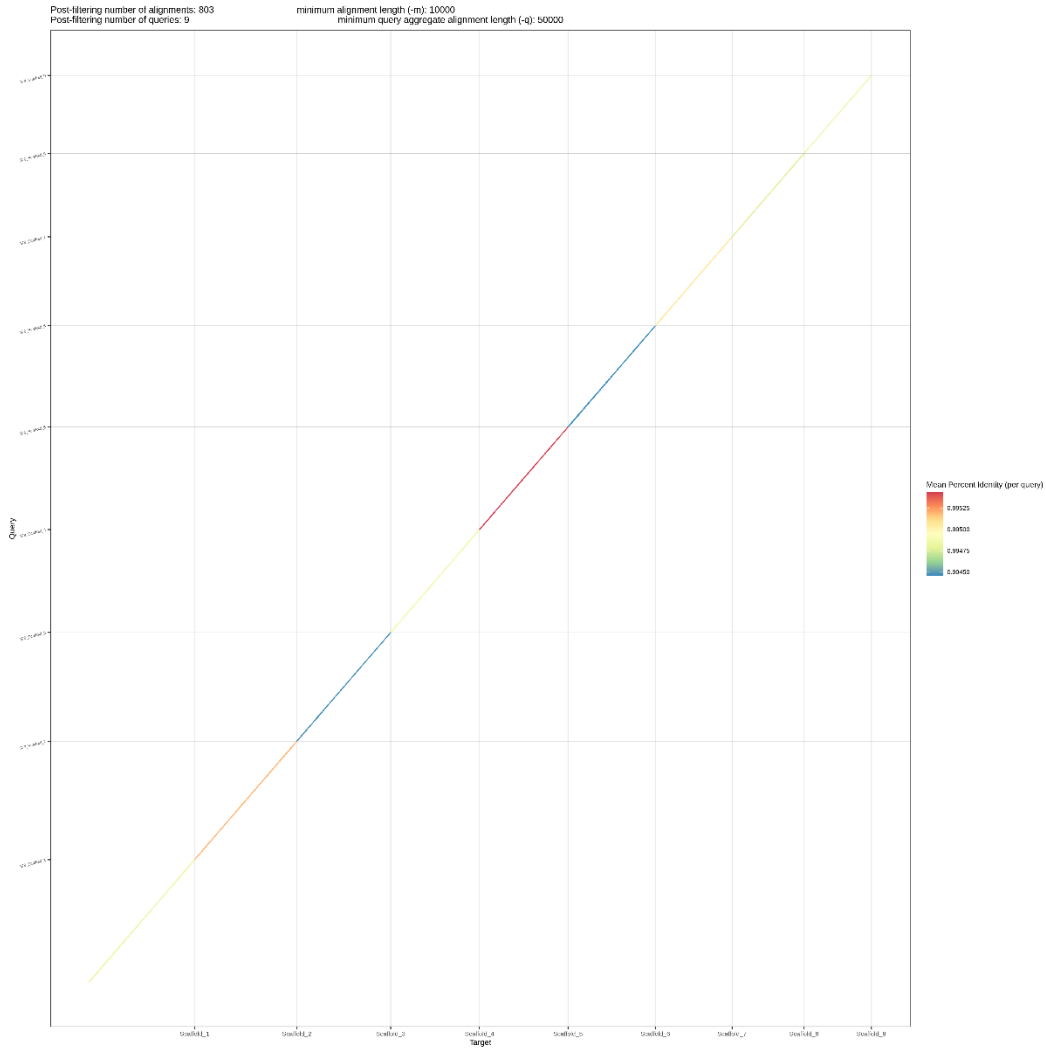


Figure 2.1 Example dot plot analysis output comparing re-sequenced individuals to reference genome. Shown above is the plot for sample 379, *Artemisia tridentata* ssp. *tridentata* from population NVW1 in Nevada. All dot plot analyses inferred high similarity across all pseudo-chromosome scaffolds, as can be seen by the unbroken diagonal line and less than 1% difference found at all levels. There were also no large chromosomal rearrangements. The rest of the samples' dot plots can be found in supplementary material.

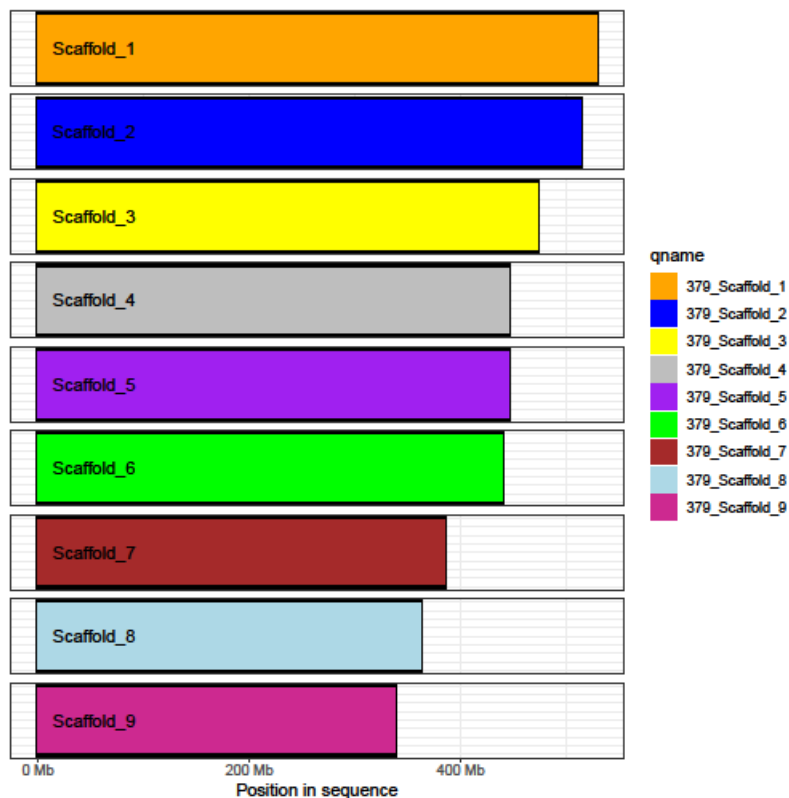


Figure 2.2 Genome coverage map comparing sample 379 with the reference genome. No large chromosomal rearrangements were found. All samples were found to have similar plots with appropriate genome coverage. The other samples' coverage maps can be found in supplementary materials.

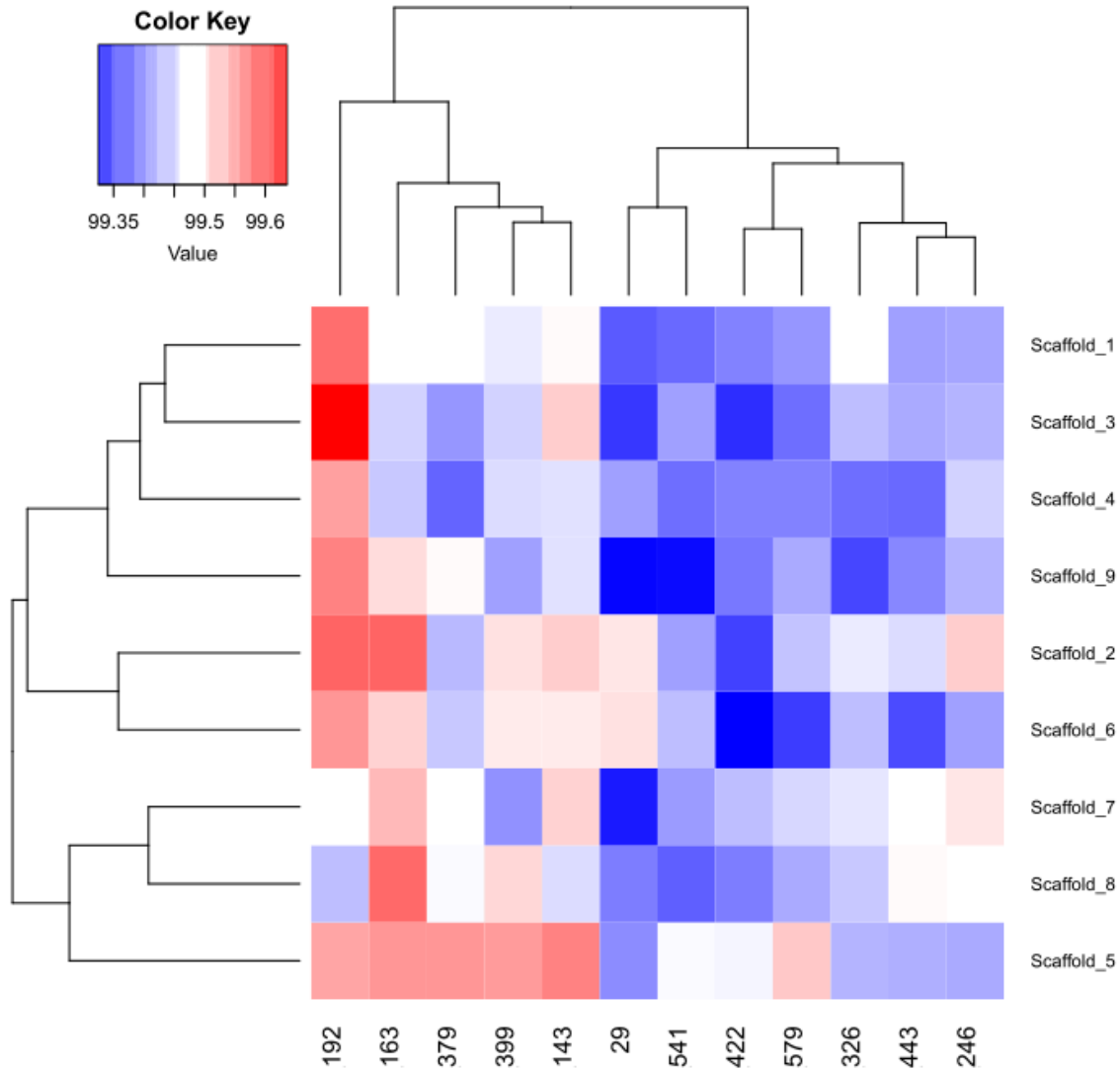


Figure 2.3 Heatmap comparing samples with the reference genome at the pseudo-chromosome level. We found high levels of similarity between the reference genome and all samples; less than 1% difference was inferred. Samples did not segregate directly into populations.

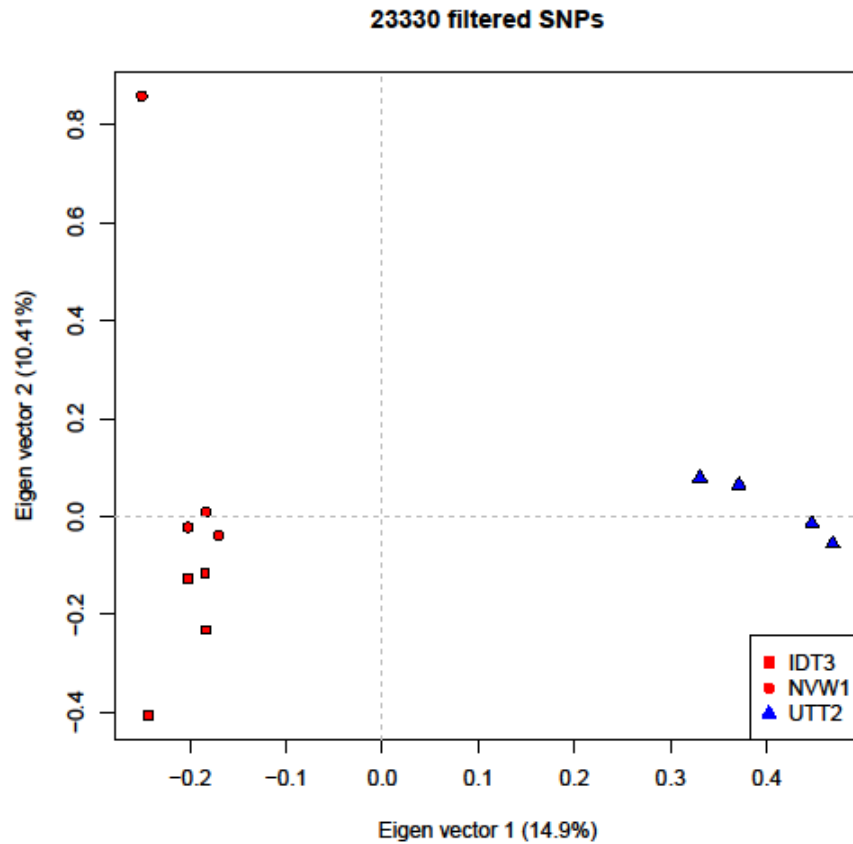


Figure 2.4 Principal Component Analysis (PCA) of filtered biallelic single nucleotide polymorphisms (SNPs) of diploid basin sagebrush seedlings (*Artemisia tridentata* ssp. *tridentata*). The top eigenvector segregated our twelve seedlings following the same division as previous climatic and phenotypic analyses at the population level.

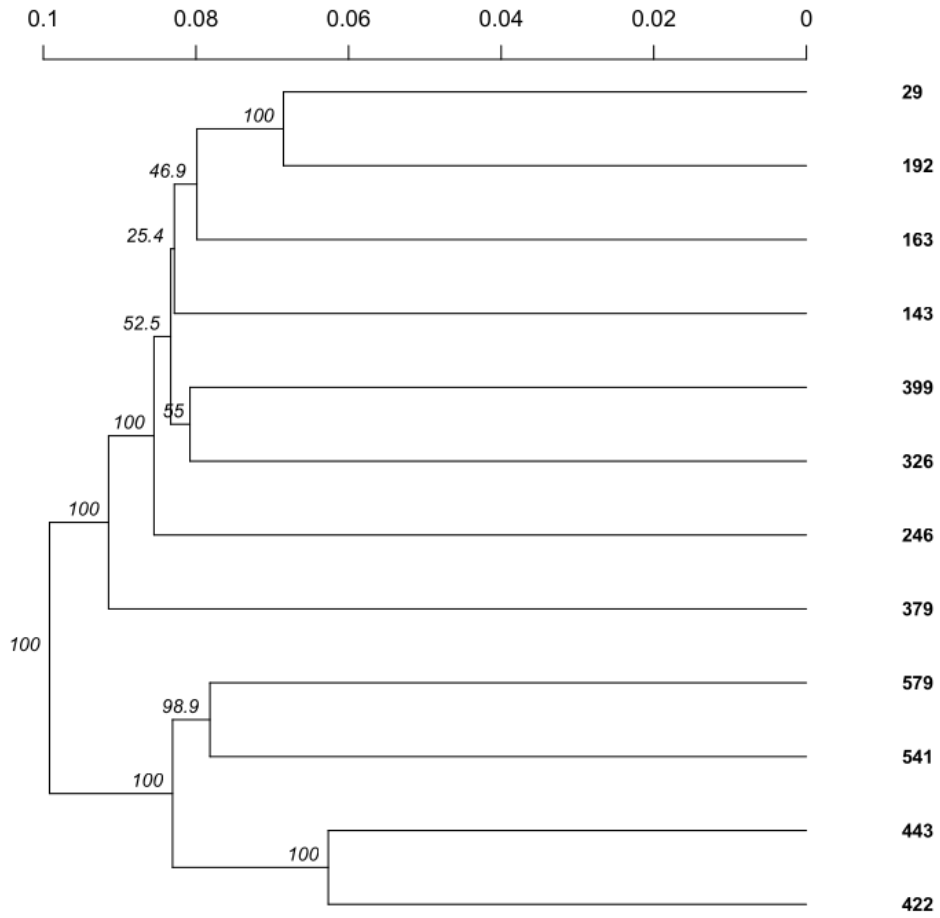


Figure 2.5 Dendrogram with bootstrap support showing genetic distance differentiation. Sample IDs are at the terminal ends of branches. Genetic differentiation was calculated using Nei's distance (1987). Branching between seedlings from population UTT2 and the rest was supported- bootstrap value 100.

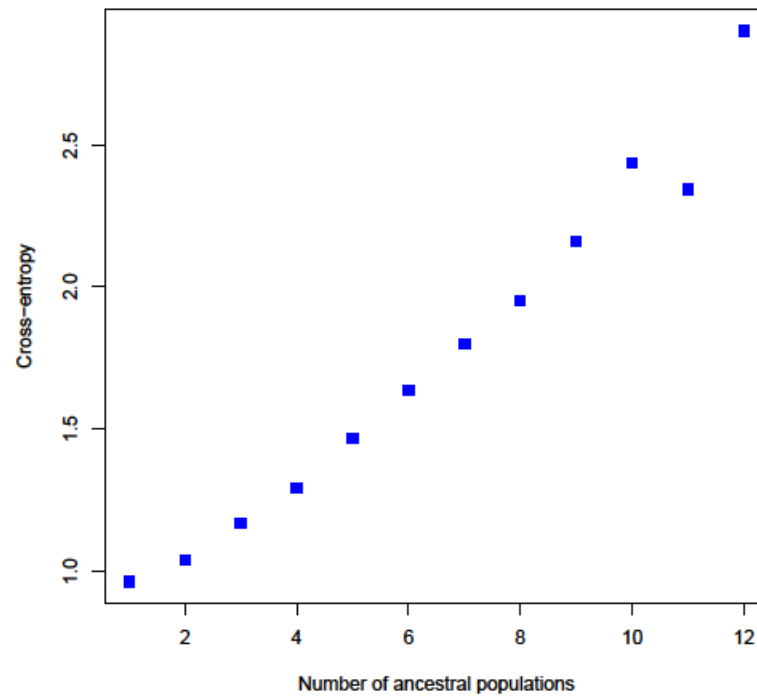


Figure 2.6 Cross Entropy plot output from STRUCTURE analysis. The STRUCTURE analysis indicated that one ancestral meta-population was the most likely scenario to explain the neutral SNP variation in our dataset, as seen by scenario 1 having the lowest cross-entropy value.

REFERENCES

- Adams, D.K., & Comrie, A.C. (1997). The North American Monsoon. *Bulletin of the American Meteorological Society*, American Meteorological Society. Accessed 17 March 2023.
- Aitken, S. N., Yeaman, S., Holliday, J. A., Wang, T., & Curtis-McLane, S. (2008). Adaptation, migration or extirpation: climate change outcomes for tree populations. *Evolutionary applications*, 1(1), 95–111.
<https://doi.org/10.1111/j.1752-4571.2007.00013.x>
- Allsman, L., Dieffenbacher, R., & Rasmussen, C. (2019). Glue Impressions of Maize Leaves and Their Use in Classifying Mutants. *BIO-PROTOCOL*, 9(7).
<https://doi.org/10.21769/BioProtoc.3209>
- Andrews, S. (2010). FastQC: A Quality Control Tool for High Throughput Sequence Data [Online]. Available online at:
<http://www.bioinformatics.babraham.ac.uk/projects/fastqc/>
- Arango-Velez, A., Zwiazek, J.J., Thomas, B.R. and Tyree, M.T. (2011), Stomatal factors and vulnerability of stem xylem to cavitation in poplars. *Physiologia Plantarum*, 143: 154-165. <https://doi.org/10.1111/j.1399-3054.2011.01489.x>
- Bertolino, L. T., Caine, R. S., & Gray, J. E. (2019). Impact of Stomatal Density and Morphology on Water-Use Efficiency in a Changing World. *Frontiers in Plant Science*, 10, 225. <https://doi.org/10.3389/fpls.2019.00225>
- Bímová, A. (1992). Heterogeneity of stomatal density in the second wheat leaf. *Biologia Plantarum*, 34(5–6). <https://doi.org/10.1007/BF02923606>
- Bhaskara, G. B., Lasky, J. R., Razzaque, S., Zhang, L., Haque, T., Bonnette, J. E., Civelek, G. Z., Verslues, P. E., & Juenger, T. E. (2022). Natural variation identifies new effectors of water-use efficiency in *Arabidopsis*. *Proceedings of the National Academy of Sciences of the United States of America*, 119(33), e2205305119. <https://doi.org/10.1073/pnas.2205305119>
- Bímová, A. (1992). Heterogeneity of stomatal density in the second wheat leaf. *Biologia Plantarum*, 34(5–6). <https://doi.org/10.1007/BF02923606>

- Bolger, A.M., Lohse, M., Usadel, B., Trimmomatic: a flexible trimmer for Illumina sequence data, *Bioinformatics*, Volume 30, Issue 15, August 2014, Pages 2114–2120, <https://doi.org/10.1093/bioinformatics/btu170>
- Boos, W.R., Pascale, S. (2021). Mechanical forcing of the North American monsoon by orography. *Nature* 599, 611–615. <https://doi.org/10.1038/s41586-021-03978-2>
- Casablanca, T., Lachmuth, S., Fitzpatrick, M. C., & Keller, S. R. (2023). From common gardens to candidate genes: exploring local adaptation to climate in red spruce. *The New phytologist*, 237(5), 1590–1605. <https://doi.org/10.1111/nph.18465>
- Chaney, L., Richardson, B. A., & Germino, M. J. (2017). Climate drives adaptive genetic responses associated with survival in big sagebrush (*Artemisia tridentata*). *Evolutionary Applications*, 10(4), 313–322. <https://doi.org/10.1111/eva.12440>
- Chen, G., Wang, Y., Wang, X., Yang, Q., Quan, X., Zeng, J., Dai, F., Zeng, F., Wu, F., Zhang, G., & Chen, Z.-H. (2019). Leaf epidermis transcriptome reveals drought-induced hormonal signaling for stomatal regulation in wild barley. *Plant Growth Regulation*, 87(1), 39–54. <https://doi.org/10.1007/s10725-018-0450-0>
- Comas, L. H., Becker, S. R., Cruz, V. M. V., Byrne, P. F., & Dierig, D. A. (2013). Root traits contributing to plant productivity under drought. *Frontiers in Plant Science*, 4. <https://doi.org/10.3389/fpls.2013.00442>
- Coop, J. D., Parks, S. A., Stevens-Rumann, C. S., Crausbay, S. D., Higuera, P. E., Hurteau, M. D., Tepley, A., Whitman, E., Assal, T., Collins, B. M., Davis, K. T., Dobrowski, S., Falk, D. A., Fornwalt, P. J., Fulé, P. Z., Harvey, B. J., Kane, V. R., Littlefield, C. E., Margolis, E. Q., ... Rodman, K. C. (2020). Wildfire-Driven Forest Conversion in Western North American Landscapes. *BioScience*, 70(8), 659–673. <https://doi.org/10.1093/biosci/biaa061>
- Dittberner, H., Korte, A., Mettler-Altmann, T., Weber, A. P. M., Monroe, G., & de Meaux, J. (2018). Natural variation in stomata size contributes to the local adaptation of water-use efficiency in *Arabidopsis thaliana*. *Molecular Ecology*, 27(20), 4052–4065. <https://doi.org/10.1111/mec.14838>

- Downs, J.L., & Black, R.A. (1999). Leaf Surface Characteristics and Gas Exchange in *Artemisia tridentata* subspecies *wyomingensis* and *tridentata*. USDA Forest Service Proceedings RMRS-P-11. 108-112.
- Drake, P. L., Froend, R. H., & Franks, P. J. (2013). Smaller, faster stomata: Scaling of stomatal size, rate of response, and stomatal conductance. *Journal of Experimental Botany*, 64(2), 495–505. <https://doi.org/10.1093/jxb/ers347>
- Dunn, J., Hunt, L., Afsharinafar, M., Meselmani, M. A., Mitchell, A., Howells, R., Wallington, E., Fleming, A. J., & Gray, J. E. (2019). Reduced stomatal density in bread wheat leads to increased water-use efficiency. *Journal of Experimental Botany*, 70(18), 4737–4748. <https://doi.org/10.1093/jxb/erz248>
- Eisele, J. F., Fäßler, F., Bürgel, P. F., & Chaban, C. (2016). A Rapid and Simple Method for Microscopy-Based Stomata Analyses. *PLOS ONE*, 11(10), e0164576. <https://doi.org/10.1371/journal.pone.0164576>
- Eisenach, C., Chen, Z., Grefen, C., & Blatt, M. R. (2012). The trafficking protein SYP121 of *Arabidopsis* connects programmed stomatal closure and K⁺ channel activity with vegetative growth. *The Plant Journal*, 69(2), 241–251. <https://doi.org/10.1111/j.1365-313X.2011.04786.x>
- Elfarargi, A. F., Gilbault, E., Döring, N., Neto, C., Fulgione, A., Weber, A. P. M., Loudet, O., & Hancock, A. M. (2023). Genomic Basis of Adaptation to a Novel Precipitation Regime. *Molecular biology and evolution*, 40(3), msad031. <https://doi.org/10.1093/molbev/msad031>
- Evans, L. S., & Graney, H. J. (2018). Quantification of concavities in roots of *Artemisia tridentata*. *Rhizosphere*, 6, 52–55. <https://doi.org/10.1016/j.rhisph.2018.03.001>
- Evans, L. S., Kharran, T. A., Pena, I., & Kitchen, S. G. (2019). Quantification of Eccentricity in Stems of *Artemisia tridentata* Nutt. *Western North American Naturalist*, 79(3), 441. <https://doi.org/10.3398/064.079.0312>
- Fang, Y., & Xiong, L. (2015). General mechanisms of drought response and their application in drought resistance improvement in plants. *Cellular and Molecular Life Sciences*, 72(4), 673–689. <https://doi.org/10.1007/s00018-014-1767-0>

- Faske, T. M., Agneray, A. C., Jahner, J. P., Sheta, L. M., Leger, E. A., & Parchman, T. L. (2021). Genomic and common garden approaches yield complementary results for quantifying environmental drivers of local adaptation in rubber rabbitbrush, a foundational Great Basin shrub. *Evolutionary Applications*, 14(12), 2881–2900. <https://doi.org/10.1111/eva.13323>
- Faralli, M., Matthews, J., & Lawson, T. (2019). Exploiting natural variation and genetic manipulation of stomatal conductance for crop improvement. *Current Opinion in Plant Biology*, 49, 1–7. <https://doi.org/10.1016/j.pbi.2019.01.003>
- Franks, P.J., W. Doheny-Adams, T., Britton-Harper, Z.J. and Gray, J.E. (2015), Increasing water-use efficiency directly through genetic manipulation of stomatal density. *New Phytol*, 207: 188-195. <https://doi.org/10.1111/nph.13347>
- Franks, S.J., & Hoffman, A.A. (2012). Genetics of Climate Adaptation. *Annu. Rev. Genet.* 2012. 46:185–208. DOI: 10.1146/annurev-genet-110711-155511
- Frichot E, Francois O (2015). “LEA: an R package for Landscape and Ecological Association studies.” *Methods in Ecology and Evolution*. <http://membres-timc.imag.fr/Olivier.Francois/lea.html>.
- Ginzburg, C. (1963). Some anatomic features of splitting of desert shrubs. *Phytomorphology* 13, 92-97.
- Gupta, A., Rico-Medina, A., & Caño-Delgado, A. I. (2020). The physiology of plant responses to drought. *Science*, 368(6488), 266–269. <https://doi.org/10.1126/science.aaz7614>
- Hartman, G., & Danin, A. (2010). Isotopic values of plants in relation to water availability in the Eastern Mediterranean region. *Oecologia*, 162(4), 837–852. <https://doi.org/10.1007/s00442-009-1514-7>
- Hughes, J., Hepworth, C., Dutton, C., Dunn, J. A., Hunt, L., Stephens, J., Waugh, R., Cameron, D. D., & Gray, J. E. (2017). Reducing Stomatal Density in Barley Improves Drought Tolerance without Impacting on Yield. *Plant Physiology*, 174(2), 776–787. <https://doi.org/10.1104/pp.16.01844>

- IPCC, 2022: Summary for Policymakers [H.-O. Pörtner, D.C. Roberts, E.S. Poloczanska, K. Mintenbeck, M. Tignor, A. Alegría, M. Craig, S. Langsdorf, S. Lösschke, V. Möller, A. Okem (eds.)]. In: *Climate Change 2022: Impacts, Adaptation, and Vulnerability. Contribution of Working Group II to the Sixth Assessment Report of the Intergovernmental Panel on Climate Change* [H.-O. Pörtner, D.C. Roberts, M. Tignor, E.S. Poloczanska, K. Mintenbeck, A. Alegría, M. Craig, S. Langsdorf, S. Lösschke, V. Möller, A. Okem, B. Rama (eds.)]. Cambridge University Press, Cambridge, UK and New York, NY, USA, pp. 3-33, doi:10.1017/9781009325844.001.
- IUCN. 2022. The IUCN Red List of Threatened Species. Version 2022-2. <https://www.iucnredlist.org>. Accessed on [1 February 2023].
- Kamvar, Z. N., Brooks, J. C., & Grünwald, N. J. (2015). Novel R tools for analysis of genome-wide population genetic data with emphasis on clonality. *Frontiers in genetics*, 6, 208. <https://doi.org/10.3389/fgene.2015.00208>
- Kannenbergh, S. A., Driscoll, A. W., Szejner, P., Anderegg, W. R. L., & Ehleringer, J. R. (2021). Rapid increases in shrubland and forest intrinsic water-use efficiency during an ongoing megadrought. *Proceedings of the National Academy of Sciences*, 118(52), e2118052118. <https://doi.org/10.1073/pnas.2118052118>
- Kardiman, R., & Ræbild, A. (2018). Relationship between stomatal density, size and speed of opening in Sumatran rainforest species. *Tree Physiology*, 38(5), 696–705. <https://doi.org/10.1093/treephys/tpx149>
- Knaus, Brian J., and Niklaus J. Grunwald. (2017). VCFR: a package to manipulate and visualize variant call format data in R. *Molecular Ecology Resources* 17(1):44-53. <http://dx.doi.org/10.1111/1755-0998.12549>.
- Knick, S. T., Dobkin, D. S., Rotenberry, J. T., Schroeder, M. A., Vander Haegen, W. M., & van Riper, C. (2003). Teetering on the Edge or too Late? Conservation and Research Issues for Avifauna of Sagebrush Habitats. *The Condor*, 105(4), 611–634. <https://doi.org/10.1093/condor/105.4.611>

- Kruskal, W.H. & Wallis, W.A., (1952) Use of Ranks in One-Criterion Variance Analysis, *Journal of the American Statistical Association*, 47:260, 583-621, DOI: 10.1080/01621459.1952.10483441
- Kubínová, L. (1994). Recent stereological methods for measuring leaf anatomical characteristics: Estimation of the number and sizes of stomata and mesophyll cells. *Journal of Experimental Botany*, 45(1), 119–127. <https://doi.org/10.1093/jxb/45.1.119>
- Langmead B, Salzberg SL. Fast gapped-read alignment with Bowtie 2. *Nat Methods*. 2012 Mar 4;9(4):357-9. doi: 10.1038/nmeth.1923. PMID: 22388286; PMCID: PMC3322381.
- Lu J., Ge, S., McNulty, S., and Amatya, D.M. (2005). A Comparison of Six Potential Evapotranspiration Methods for Regional Use in the Southeastern United States. *Journal of the American Water Resources Association (JAWRA)* 41 (3):621-633.
- Maier, A. M., Perryman, B. L., Olson, R. A., & Hild, A. L. (2001). Climatic Influences on Recruitment of 3 Subspecies of *Artemisia tridentata*. *Journal of Range Management*, 54(6), 699. <https://doi.org/10.2307/4003674>
- Mano, N. A., Madore, B., & Mickelbart, M. V. (2023). Different Leaf Anatomical Responses to Water Deficit in Maize and Soybean. *Life*, 13(2), 290. <https://doi.org/10.3390/life13020290>
- McDowell, N., Pockman, W. T., Allen, C. D., Breshears, D. D., Cobb, N., Kolb, T., Plaut, J., Sperry, J., West, A., Williams, D. G., & Yezzer, E. A. (2008). Mechanisms of plant survival and mortality during drought: Why do some plants survive while others succumb to drought? *New Phytologist*, 178(4), 719–739. <https://doi.org/10.1111/j.1469-8137.2008.02436.x>
- McElrone, A. J., Pockman, W. T., Martínez-Vilalta, J., & Jackson, R. B. (2004). Variation in xylem structure and function in stems and roots of trees to 20 m depth. *New Phytologist*, 163(3), 507–517. <https://doi.org/10.1111/j.1469-8137.2004.01127.x>

- Melton, A. E., Beck, J., Galla, S. J., Jenkins, J., Handley, L., Kim, M., Grimwood, J., Schmutz, J., Richardson, B. A., Serpe, M., Novak, S., & Buerki, S. (2021). A draft genome provides hypotheses on drought tolerance in a keystone plant species in Western North America threatened by climate change. *Ecology and evolution*, 11(21), 15417–15429. <https://doi.org/10.1002/ece3.8245>
- Melton, A. E., Child, A. W., Beard, R. S., Dumaguit, C. D. C., Forbey, J. S., Germino, M., de Graaff, M.-A., Kliskey, A., Leitch, I. J., Martinez, P., Novak, S. J., Pellicer, J., Richardson, B. A., Self, D., Serpe, M., & Buerki, S. (2022). A haploid pseudo-chromosome genome assembly for a keystone sagebrush species of western North American rangelands. *G3 Genes|Genomes|Genetics*, 12(7), jkac122. <https://doi.org/10.1093/g3journal/jkac122>
- Melton, A. E., Moran, K., Martinez, P., Ellestad, P., Milliken, E., Morales, W., Child, A.W., Richardson, B.A., Serpe, M., Novak, S.J., & Buerki, S. (2023) A Genotype×Environment experiment reveals contrasting response strategies to drought between populations of a keystone species (*Artemisia tridentata*; Asteraceae). *Plant-Environment Interactions*. Manuscript in Review. Submitted March 2, 2023.
- Meng, L.-S. (2018). Compound Synthesis or Growth and Development of Roots/Stomata Regulate Plant Drought Tolerance or Water Use Efficiency/Water Uptake
- Munjonji L., & Ayisi, L.K. (2021). Leaf gas exchange and $\delta^{13}\text{C}$ in cowpea and triticale under water stress and well-watered conditions, *Heliyon*, Volume 7, Issue 5, e07060, ISSN 2405-8440, <https://doi.org/10.1016/j.heliyon.2021.e07060>.
- Efficiency. *Journal of Agricultural and Food Chemistry*, 66(14), 3595–3604. <https://doi.org/10.1021/acs.jafc.7b05990>
- Munjonji, L., Ayisi, K.K. (2021). Leaf gas exchange and $\delta^{13}\text{C}$ in cowpea and triticale under water stress and well-watered conditions, *Heliyon*, Volume 7, Issue 5, e07060, ISSN 2405-8440, <https://doi.org/10.1016/j.heliyon.2021.e07060>.
- Navock, Kara A., "Phenotypic Responses of Sagebrush to the Southwestern North America Megadrought: A Genotype-by-Environment (GxE) Approach" (2020).

Boise State University Theses and Dissertations. 1772.

10.18122/td/1772/boisestate

- Ofori, B. Y., Stow, A. J., Baumgartner, J. B., & Beaumont, L. J. (2017). Influence of adaptive capacity on the outcome of climate change vulnerability assessment. *Scientific Reports*, 7(1), 12979. <https://doi.org/10.1038/s41598-017-13245-y>
- Oladosu, Y., Rafii, M. Y., Samuel, C., Fatai, A., Magaji, U., Kareem, I., Kamarudin, Z. S., Muhammad, I., & Kolapo, K. (2019). Drought Resistance in Rice from Conventional to Molecular Breeding: A Review. *International Journal of Molecular Sciences*, 20(14), 3519. <https://doi.org/10.3390/ijms20143519>
- Paccard, A., Fruleux, A., & Willi, Y. (2014). Latitudinal trait variation and responses to drought in *Arabidopsis lyrata*. *Oecologia*, 175(2), 577587. <https://doi.org/10.1007/s00442-014-2932-8>
- Paradis E. (2010). pegas: an R package for population genetics with an integrated–modular approach. *Bioinformatics* 26: 419–420. doi:10.1093/bioinformatics/btp696.
- Pazourek, J. (1973). The density of stomata in leaves of different ecotypes of *Phragmites communis*. *Folia Geobotanica & Phytotaxonomica*, 8(1), 15–21. <https://doi.org/10.1007/BF02854680>
- Perryman, B. L., Maier, A. M., Hild, A. L., & Olson, R. A. (2001). Demographic Characteristics of 3 *Artemisia tridentata* Nutt. Subspecies. *Journal of Range Management*, 54(2), 166. <https://doi.org/10.2307/4003178>
- Remington TE, Deibert PA, Hanser SE, Davis DM, Robb LA, L WJ. (2021). Sagebrush conservation strategy—challenges to sagebrush conservation: U.S. Geological Survey Open-File Report 2020–1125, p. 327. <https://doi.org/10.3133/ofr20201125>.
- Richardson, B.A., Page, J.T., Bajgain, P., Sanderson, S.C. and Udall, J.A. (2012), Deep sequencing of amplicons reveals widespread intraspecific hybridization and multiple origins of polyploidy in big sagebrush (*Artemisia tridentata*; Asteraceae). *American Journal of Botany*, 99: 1962-1975. <https://doi.org/10.3732/ajb.1200373>

- Rigge M, Homer C, Cleeves L, Meyer DK, Bunde B, Shi H, Xian G, Schell S, Bobo M. (2020). Quantifying Western U.S. Rangelands as Fractional Components with Multi-Resolution Remote Sensing and In Situ Data. *Remote Sensing*. 12(3):412. <https://doi.org/10.3390/rs12030412>
- Rumman, R, Atkin, OK, Bloomfield, KJ, Eamus, D. (2017) Variation in bulk-leaf ^{13}C discrimination, leaf traits and water-use efficiency–trait relationships along a continental-scale climate gradient in Australia. *Glob Change Biol*. 2018; 24: 1186–1200. <https://doi.org/10.1111/gcb.13911>
- Savolainen, Outi & Lascoux, Martin & Merilä, Juha. (2013). Ecological genomics of local adaptation. *Nature reviews. Genetics*. 14. 807-20. 10.1038/nrg3522.
- Schenk, H. J. (1999). Clonal splitting in desert shrubs. *Plant Ecology*, 141(1/2), 41–52. <https://doi.org/10.1023/A:1009895603783>
- Schenk, H. J., Espino, S., Goedhart, C. M., Nordenstahl, M., Cabrera, H. I. M., & Jones, C. S. (2008). Hydraulic integration and shrub growth form linked across continental aridity gradients. *Proceedings of the National Academy of Sciences*, 105(32), 11248–11253. <https://doi.org/10.1073/pnas.0804294105>
- Schindelin, J., Arganda-Carreras, I., Frise, E., Kaynig, V., Longair, M., Pietzsch, T., ... Cardona, A. (2012). Fiji: an open-source platform for biological-image analysis. *Nature Methods*, 9(7), 676–682. doi:10.1038/nmeth.2019
- Seibt, U., Rajabi, A., Griffiths, H. et al. (2008). Carbon isotopes and water use efficiency: sense and sensitivity. *Oecologia* 155, 441–454. <https://doi.org/10.1007/s00442-007-0932-7>
- da Silva, N. R., Oliveira, M. W. da S., Filho, H. A. de A., Pinheiro, L. F. S., Rossatto, D. R., Kolb, R. M., & Bruno, O. M. (2016). Leaf epidermis images for robust identification of plants. *Scientific Reports*, 6(1), 25994. <https://doi.org/10.1038/srep25994>
- Slavík, B. (1963). The distribution pattern of transpiration rate, water saturation deficit, stomata number and size, photosynthetic and respiration rate in the area of the

- tobacco leaf blade. *Biologia Plantarum*, 5(2), 143–153.
<https://doi.org/10.1007/BF02933646>
- Stahle, D. W. (2020). Anthropogenic megadrought. *Science*, 368(6488), 238-239. DOI: 10.1126/science.abb6902
- Stojnić, S., Suchocka, M., Benito-Garzón, M., Torres-Ruiz, J. M., Cochard, H., Bolte, A., Coccozza, C., Cvjetković, B., de Luis, M., Martinez-Vilalta, J., Ræbild, A., Tognetti, R., & Delzon, S. (2018). Variation in xylem vulnerability to embolism in European beech from geographically marginal populations. *Tree Physiology*, 38(2), 173–185. <https://doi.org/10.1093/treephys/tpx128>
- Uffelmann, E., Huang, Q.Q., Munung, N.S. et al. Genome-wide association studies. *Nat Rev Methods Primers* 1, 59 (2021). <https://doi.org/10.1038/s43586-021-00056-9>
- Urban, M.C., et al., (2016). Improving the forecast for biodiversity under climate change. *Science*, 353, aad8466. DOI:10.1126/science.aad8466
- Vantyghem, M., Merckx, R., Stevens, B., Hood-Nowotny, R., Swennen, R., & Dercon, G. (2021). The potential of stable carbon isotope ratios and leaf temperature as proxies for drought stress in banana under field conditions. *Agricultural Water Management*, Volume 260, 107247, ISSN 0378-3774, <https://doi.org/10.1016/j.agwat.2021.107247>.
- de Villemereuil, P., Gaggiotti, O. E., Mouterde, M., & Till-Bottraud, I. (2016). Common garden experiments in the genomic era: New perspectives and opportunities. *Heredity*, 116(3), 249–254. <https://doi.org/10.1038/hdy.2015.93>
- Wang, Y., Papanatsiou, M., Eisenach, C., Karnik, R., Williams, M., Hills, A., Lew, V. L., & Blatt, M. R. (2012). Systems Dynamic Modeling of a Guard Cell Cl⁻ Channel Mutant Uncovers an Emergent Homeostatic Network Regulating Stomatal Transpiration. *Plant Physiology*, 160(4), 1956–1967.
<https://doi.org/10.1104/pp.112.207704>
- Williams, A. P., Cook, E. R., Smerdon, J. E., Cook, B. I., Abatzoglou, J. T., Bolles, K., Baek, S. H., Badger, A. M., & Livneh, B. (2020). Large contribution from

- anthropogenic warming to an emerging North American megadrought. *Science*, 368(6488), 314–318. <https://doi.org/10.1126/science.aaz9600>
- Wu, F.-H., Shen, S.-C., Lee, L.-Y., Lee, S.-H., Chan, M.-T., & Lin, C.-S. (2009). Tape-Arabidopsis Sandwich—A simpler Arabidopsis protoplast isolation method. *Plant Methods*, 5(1), 16. <https://doi.org/10.1186/1746-4811-5-16>
- Xu, Y., Ramanathan, V., & Victor, D.G. (2018) Global warming will happen faster than we think. *Nature*, 30-32. doi: <https://doi.org/10.1038/d41586-018-07586-5>
- Zhang, L., Niu, H., Wang, S., Zhu, X., Luo, C., Li, Y., & Zhao, X. (2012). Gene or environment? Species-specific control of stomatal density and length: Species-Specific Control of SD and SL. *Ecology and Evolution*, 2(5), 1065–1070. <https://doi.org/10.1002/ece3.23>